Design and Development of Low-cost Multi-function UAV Suitable for Production and Operation in Low Resource Environments

By: Zachary Dakotah Standridge

Thesis submitted to the faculty of the
Virginia Polytechnic Institute and State University in partial
fulfillment of the requirements for the degree of

Master of Science
In
Aerospace Engineering

Kevin Kochersberger, Co-Chair
Pradeep Raj, Co-Chair
William Mason

May 8, 2018
Blacksburg, VA

Keywords: Rapid Prototyping, Developing Country, Posterboard Wings, UAV Design, Range Optimization

Design and Development of Low-cost Multi-function UAV Suitable for Production and Operation in Low Resource Environments

By: Zachary Dakotah Standridge

ABSTRACT

A new flying wing design has been developed at the Unmanned Systems Lab (USL) at Virginia Tech to serve delivery and remote sensing applications in the developing world. The fully autonomous unmanned aerial vehicle (UAV), named EcoSoar, was designed with the goal of creating a business opportunity for local entrepreneurs in low-resource communities. The system was developed in such a way that local fabrication, operation, and maintenance of the aircraft are all possible. In order to present a competitive financial model for sustained drone services, EcoSoar is made with reliable low-cost materials and electronics. This paper lays out the rapid prototyping and flight experiment efforts that went into polishing the design, test results from an EcoSoar centered drone workshop in Kasungu, Malawi, and finally a range optimization study with flight test validation.

Design and Development of Low-cost Multi-function UAV Suitable for Production and Operation in Low Resource Environments

By: Zachary Dakotah Standridge

GENERAL AUDIENCE ABSTRACT

A new humanitarian drone has been developed at the Unmanned Systems Lab (USL) at Virginia Tech. The unmanned aerial vehicle (UAV), named EcoSoar, was designed with the goal of creating a business opportunity for local entrepreneurs in low-resource communities. In order to be a viable solution in the developing world EcoSoar utilizes customizable 3D-printed parts and wings made from cheap materials like posterboard and packing tape. In addition, tools for building the drone have been developed in such a way that anyone can learn to construct and operate EcoSoar regardless of experience. This paper lays out the engineering efforts that went into the design, lessons learned from an EcoSoar-centered workshop in Kasungu, Malawi, and finally offers an upgraded design.

Acknowledgements

I'd like to express my gratitude for the many people who have had major impacts on my graduate experience. First off, a big thank you to Dr. K who - for some reason - hired me as an undergraduate even though I scarcely had experience. I don't think I would be able to credit myself an engineer without the invaluable skills I've gained by tinkering about in the Unmanned Systems Lab.

Speaking of the USL, I really have to commend our Lab Technician Andrew Morgan for his skills in machining, piloting, manufacturing, and being able to deal with the frustration that comes with making experimental drones. And thanks for hitting me with the heavy hammer when my designs were just plain overkill. I'd also like to thank our Lab Manager, Dr. John Bird for the weekly support and offering wisdom of all kinds.

A few undergrads have really contributed to this project as well, they've been crucial in keeping my sanity after all of the early morning flight tests. James Donnelly has been a tremendous help with design iterations and sanity checking my manufacturing methods. Of course, couldn't have flown 80+ times without my top notch pilot Anthony Wagner! Thanks for keeping me company at Kentland even when the bird started flying itself. And lastly, thank you Bradley Canty for checking my math and giving another aerospace perspective in the ME dominated lab.

Contents

Chaper 1. Introduction

1.1 Business Case

UAV operations in less developed countries have been slow in adoption, although delivery and imaging capability has now progressed to a point where these applications are ideally suited for drones operating in low-resource settings. Communities with poor infrastructure especially benefit from UAV services due to the potential increase of efficiency. One example is such of emergency medical supplies, which in some countries are mostly transported on bicycles. With a proper network of low-cost UAVs lifesaving medicine could be ordered and delivered on demand.

While the applications are promising, the economics and a sustainable model for operations are more difficult to realize. Using technology that was designed for competitive markets will most likely be too expensive in less developed economies where it is common to find start-up company employees earning one USD ($1) per day. With this economic factor in mind, *EcoSoar* was designed from the ground-up to be a feasible solution for operation in low-income countries.

Several guiding principles to foster sustainable drone development and operation were referenced to guide the development of *EcoSoar*. These are shown in Table 1, and can be summarized as capacity building for UAVs being used in low-resource environments.

Table 1. Guiding principles for a sustainable drone design in low-resource environments

Principle	Feature	Value proposition
Materials must be common and easily sourced	Four 3D printed structural components and posterboard skin	The import of raw materials (plastic and foam board) is low-cost.
Support the technological literacy of the community	Airframe structure is intuitive to understand. Conventional spar/rib/skin construction assembled using a hot glue gun	Someone with no prior experience can build an airframe in two days, and learn about aircraft structures and autonomous systems technology along the way
Reduce launch and recovery complexity	Fully autonomous takeoff and landing	Aircraft does not require a pilot to operate
Robust to damage	Simple construction	Repairs are easy to make
Intuitive operational interface	Hardware is easy to program	Flight controller flight controller and Raspberry Pi camera are low-cost and open source platforms

1.2 Solution Summary

The materials used and the skill required to make *EcoSoar's* wings were the two biggest areas carefully evaluated for success in low-resource areas. Manufacturing needs boil down to a 3D printer, poster board, hot glue, and a utility knife. Production has been simplified with guides and tools developed such that someone with zero UAV experience can start fabricating and operating EcoSoar. In addition, operating procedures have been greatly minimized to reduce human factors. The vehicle is completely autonomous, power starts after being bungee launched, navigation comes from a preprogrammed mission, and when finished it simply belly lands.

EcoSoar has been refined by flight-testing over 10 aircraft, with over 50 hours of airtime. Crafting techniques for cheap materials have been mastered by rapid prototyping. 3D printed components have been integrated into aircraft for many purposes, such as modularity and repeatability in builds. The launching system has evolved from a risky hand toss to a multi-scenario bungee launch. Autonomous flight missions have been used as control experiments, where aircraft behavior and flight data have been compared across different builds to validate

design changes. *EcoSoar* is really an accumulation of an experimental approach to design engineering.

The business model was tested in Malawi, Africa where thirteen young professionals were taught how to build and operate *EcoSoar*. The trip offered many insights to developing a system for disadvantaged communities such as theirs and an amazing chance to access the shortcomings and strengths of the *EcoSoar* kit at that time. Production details often overlooked by creator bias were reviewed, ultimately improving the systems foundation. Quality checks in avionics were also added to technical documentation.

In attempt to increase the aerodynamic efficiency of the UAV platform, a range optimization study was done with a three-dimensional ideal flow solver and MATLAB's optimization toolbox. New wing geometry was found, given certain building constraints. The upgraded wings were used to create a new UAV. Flight test experiments were performed to confirm range increase and overall system effectiveness.

Chaper 2. Literature Review

2.1 Conceptual Operations for Drones in Disadvantaged Communities

The potential applications of drones in disadvantaged communities is plentiful. A fresh introduction of this technology could inspire noble engineering solutions to issues such as disease diagnostics, blood shortages, and urgent vaccination/drug needs. This list only includes payload transport missions. With the right sensors on-board, the list could definitely grow. Indigenous people know their problems more than anyone, and with this new technology as a tool more solutions are bound to come up.

2.1.1 Small Payload Transport

Many regions with poor infrastructure do not have reliable ground transportation systems, especially villages that can only be reached by bicycle or foot. Where there are roads, they are likely made of dirt or riddled with potholes. This makes vehicle transportation of time critical or temperature sensitive items challenging. A drone can take the shortest path over any terrain from point A to point B, saving time and reducing risks that come with relying on laborers responsible for ground transportation. A study performed by Johns Hopkins University and Carnegie Mellon University used a computer simulation to analyze drone effectiveness in different situations while varying geography, population, road conditions, and vaccine schedules. The study concluded that "implementing a UAS could increase vaccine availability (96% versus 94%) and decrease costs in a wide range of settings and circumstances" (Haidari et al., 2016). By bringing drone technology to low-income-communities money, and more importantly, lives can be saved.

2.1.2 Georeferenced Aerial Imagery

Both commercial and domestic use of drones for photography and videography is becoming quite common in the United States. News media, film production, land planning, art projects, and even archaeology are all fields that already use aerial photography. The new perspective brought by drones is awe-inspiring and can be utilized for many engineering purposes.

Autonomous UAVs already use GPS data in order to find their way. Georeferenced images are easily created from the combination of this data and aerial photography. UAV missions to obtain georeferenced images are simple and allow for altitude and therefore resolution variability. Governments can map and survey infrastructure to locate anomalies like road potholes or downed power lines. Farmers can better manage their fields by mapping and

using the data to determine plant health, ultimately increasing crop yield. Emergency services can more quickly respond to disaster relief. Technology similar to the cameras in smart phones could be used to do all of this and more.

2.1.3 Other UAS Applications

It is easy to get excited over flying aircraft collecting data to aid engineering solutions. Just look at how much media Project Wing's burrito deliveries on Virginia Tech's campus received (Nelsen & Stowe, 2016). This sort of commotion is creating a new era of drone technology. As a research facility, the Unmanned Systems Lab at Virginia Tech is always looking out for potential UAV uses. To name a few: drones to aid weather prediction, listen for certain kinds of monkeys, and even trigger lightning strikes.

In low-income-countries, UAS operations could aid potential solutions for illegal logging. Deforestation is an extreme issue for the world but those in poor areas feel the effects much closer to home. William Kamkwamba, a New York Times Bestselling author and local of Malawi, Africa has this to say on deforestation:

> *In most countries in Sub-Saharan Africa, over 90 percent of people are without electricity and use firewood for cooking and heating. In Malawi, that number is even greater. … Malawi loses more than 200 miles of forests each year, most cut down illegally by men without jobs who sell it on the roadside as firewood. … As many know, trees work like big pumping machines, sucking up the water from the earth and releasing it into the atmosphere, where it returns in the form of rain. Without the trees, this rainmaking is halted. And when there is rain, nothing is left to catch it, so it simply washes into the rivers, along with the precious topsoil and fertilizer from our maize fields, which we depend on to provide our food.* Kamkwamba and Mealer (2009)

This illegal logging is a pertinent issue with seemingly little action to prevent it. These deforestation sites could be found by integrating drones with carbon emission detectors and performing area scans. All that is required is UAV location and carbon dioxide data. Irregular

spikes of carbon dioxide in the air might indicate the use of chainsaws or other machinery used in logging. This is just one example of countless combinations that could lend a hand to humanitarian efforts around the world.

2.2 Existing UAV Solutions

Commercial air delivery systems are already here. Companies such as Amazon, Google, Matternet and Flirtey have all proven UAV transport concepts with multirotor UAS – whether it is vaccine or burrito delivery (Scott & Scott, 2017). Multirotor UAVs are heavy lifters when it comes to payload capacity; however, they are severely outclassed by fixed-wing aircraft when it comes to airspeed and range. Zipline, a California company, provides air delivery services with a fixed-wing UAS and is actively transporting medical supplies in Rwanda (Kolodny, 2016a).

The Zipline fixed-wing aircraft can travel up to 99.4 miles (160 km) at speeds of 62 mph (27.8 m/s), all while carrying a 4 lb (1.8 kg) payload (Rinaudo, 2018). A typical mission would go as follows: drop-off coordinates and autonomous flight plan are uploaded, aircraft launches from distribution center on a bungee rail system, flies along quickest route, drops payload from 40 ft (12.2 m) in the air to land within a user specified area, the bird returns to distribution center and finally lands via a tethered wire and inflatable pad. These UAVs keep in contact with a ground station over cellular network, allowing for monitoring and course changes if needed. Zipline does not provide any information regarding the cost of their aircraft, but states the cost of medical deliveries are similar to current ground solutions. (Kolodny, 2016a)

Chaper 3. Conceptual and Preliminary Design

This chapter lays out logic used in the development of *EcoSoar*. After defining requirements and choosing to develop a flying wing UAS, planform sizing was accomplished by analyzing material dimension restraints. Prototypes were made using historically successful RC

flight controller systems and aerodynamic variables from Athena Vortex Lattice (AVL) software (Drela & Youngren, 2004). Many airframe upgrades were made based off data from and observations of flight experiments, resulting in a reliable and reproducible sUAS.

3.1 Requirements

Priority design variables come from applications and operational needs in low-resource environments. Meaning the ideal UAS will fit a business model to function in developing communities. Simple missions carried out by a fixed-wing aircraft include aerial imagery and payload delivery. In the case of medicine or blood transport, a long range is needed for the system to be competitive with other solutions. When designing aircraft to maximize range the vehicle must have a high lift, low drag airframe using minimal power. In the case of aerial photography, the vehicle payload area must include room for a camera and the airspeed must allow for image overlap.

The business case requires indigenous workers to be able to build and operate *EcoSoar*; therefore, production and flight operations should be simple and intuitive. The building process and quality checks should be simple to where practically anyone can create a working aircraft. Airframe materials must be cheap enough to be appealing to the developing world – a plus would be the ability to locally source parts. Without the assurance of runways or large fields in prospective missions, the aircraft must have a portable launching system and be able to belly land on multiple terrains. A modular aircraft is also desired for easy transportation. Finally, autonomy should be maximized to reduce setup error and operator-training requirements.

3.2 Configuration

Table 2 shows a list of configurations scored on several measures of merit. The weights were determined from analyzing overall fabrication and mission requirements. To summarize, a

suitable aircraft for the business case model must be simple to manufacture and operate while fulfilling desired cost and performance characteristics.

Table 2. Decision matrix used in configuration selection

Decision Variables:	Ease of Construction	Portability	Platform Stability	Range Capability	Total weight	Ease of Design	Total Score
Weights:	**10**	**6**	**7**	**9**	**6**	**5**	
Flying Wing	9	10	4	10	8	4	336
Conventional	7	7	10	6	6	6	302
Flying Wing Bi-Plane	9.5	9	4	5	8	5	295
Boom Mounted	4	5	9	9	5	5.5	271.5
Boom Inverted V	5	6	8	9	5	6	283
V Tail	8	9	8	6	6	7	315
Tandem	6.5	8	5	7	6	4	267
Lifting Canard	4.5	8	6	7	6	5	259
Control Canard	7	8	7	8	6	3	290

With a score of 336, the flying wing configuration is chosen. By forgoing a stabilizer, the design is simplified to two wings and a fuselage. This shortens the building process and increases the modularity potential. However, this creates the challenge of developing a reproducible system that retains its stability. A flying wing is not as forgiving as conventional aircraft with a tail. In order for the unmanned aircraft to be controllable, the distant between the zero-deflection neutral point and center of gravity (CG) must be small. This means performance becomes more sensitive to changes in the vehicle's CG. Measures must be taken to ensure consistency of the CG in future builds.

3.3 Initial Sizing

Most of the planform sizing comes from restraints of using low cost materials. Coroplast and 30" x 20" posterboard were chosen as wing material due to global accessibility and use in the hobbyist community. Coroplast is waterproof corrugated plastic sheeting. Crafting techniques

allow the material to be cut and folded into wings. Posterboard, often-called foam board, has a lightweight foam filling with a paper skin. Once the paper is removed, the material becomes flimsy and can fold over on itself. To keep the production simple, the decision was made to create one wing from one piece of posterboard. Meaning, the posterboard must contain a complete 2D layout of the wing – top, bottom, and control surface. Common wing characteristics like dihedral and twist are infeasible due to the structural complexity. However, sweep, taper, and span were all considered in an iterative process of sketching and making wings. The desire to have a long span while retaining stiffness of the posterboard led to the final dimensions shown in Figures (1) and (2).

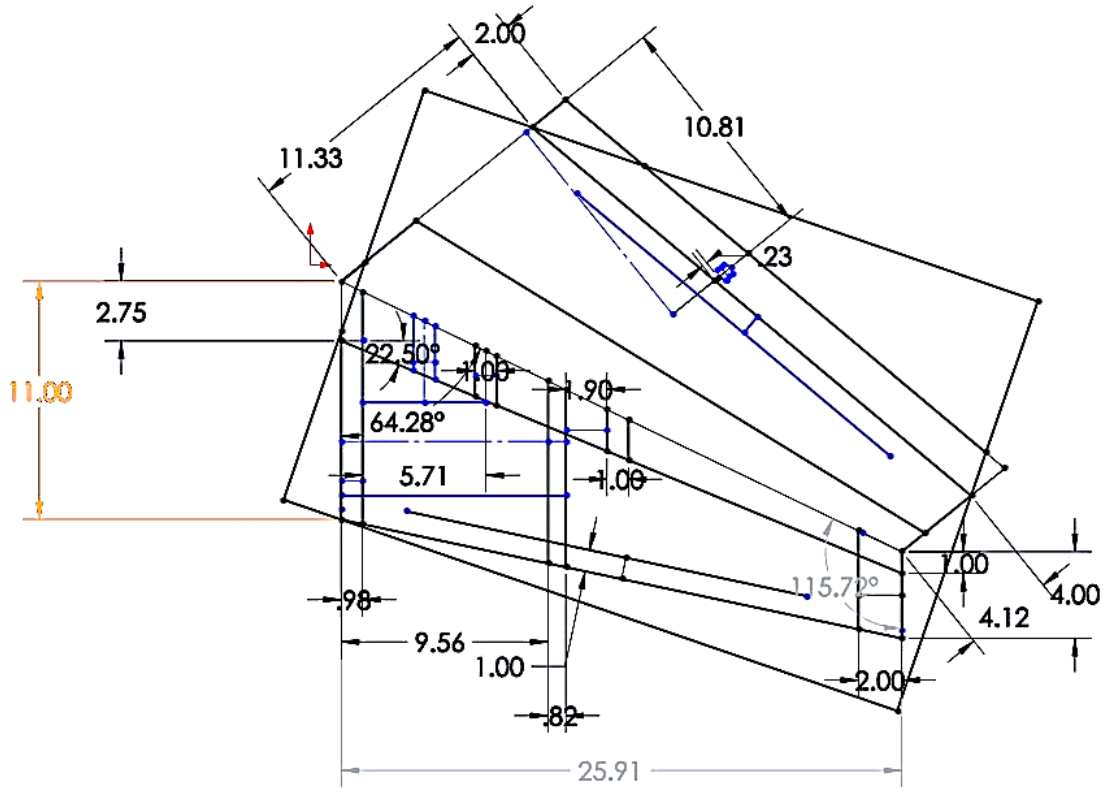

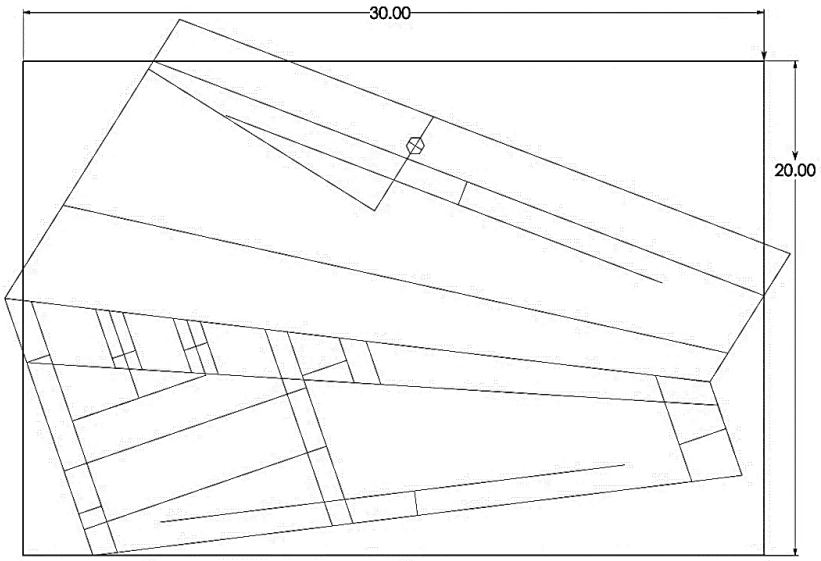

Figures 1 and 2. 2D drawings of a right wing on a 30”x20” rectangle simulating a piece of posterboard, all dimensions are inches

The drawings above shows a right wing. Simply mirroring the drawing produces the left wing. The many sketch lines are used to define details needed for production such as where to

remove paper and place 3D printed parts. Some portions of the 2D wing are strategically outside of the constrained 30”x20” space in order to maximize span and area. Once the 2D wings are cut out, folded, and attached to the fuselage the total span becomes 56.52” as showing in Figure (3).

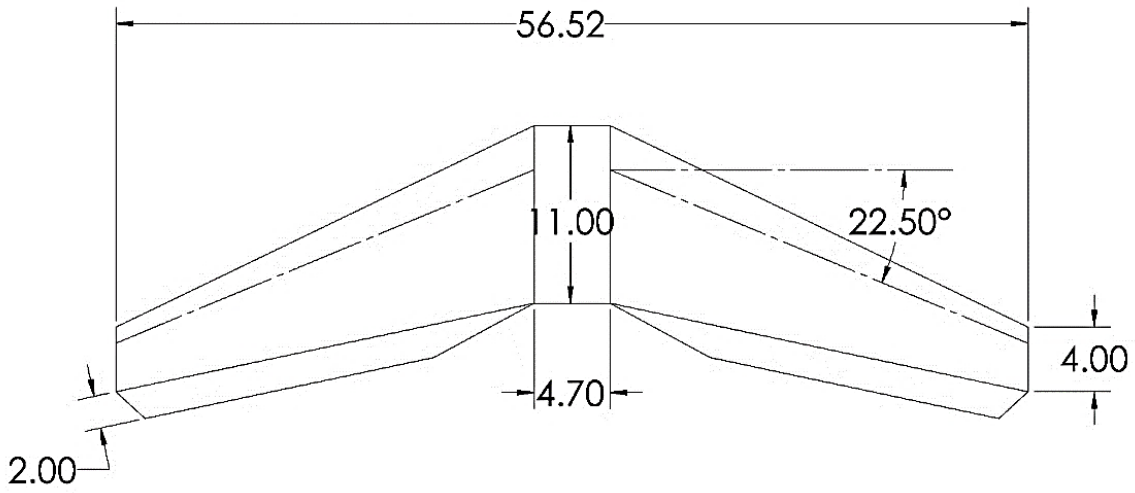

Figure 3. Top view of aircraft, showing dimensions in inches

The fuselage was sized to fit a 3”x2” flight controller and a 6”x2” battery, among other electronics needed for autonomous flight. Once the planform dimensions were known, the next goal was to obtain a total cruise weight and center of gravity estimation. AVL played a significant role in this part of the design process. As with any vortex lattice code, lifting surfaces are modeled using horseshoe vortices on a discretized geometry for numerical analysis. To create a lifting surface model and assess the capabilities of the planform, a 2D profile was needed. The cross section of flying wing prototypes can only be controlled so much – from variables such as chord length and max thickness. The resulting cross sections always have flat bottoms and moderate reflex due to the attachment area; these characteristics were taken into account when picking a 2D profile to represent the flying wing cross section. The airfoil chosen, shown in Figure (4), was a MH60 (Hepperle, 2004), a conventional flying wing airfoil with built in reflex.

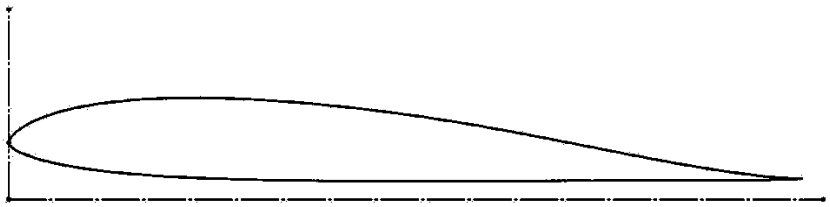

Figure 4. MH60 airfoil profile used for CAD, rotated to show near flat bottom side

The wings were modeled as AVL geometry input, Figure (5), and analyzed in force and moment equilibrium also called trim conditions. A simple flight envelope, shown in Figure (6), was created by finding the cruise angle of attack for different total weights. The desired velocity, 14 m/s, comes from being slow enough for the overlap needed to mosaic aerial imagery. The predicted maximum velocity comes from possible launch distance and acceleration needed to get the aircraft up to speed. While 18 m/s is too fast for the camera needs, it could be the cruise velocity for delivery missions. The stall angle of 10° is a precautionary value for crafted wings. For a Reynold's number (Re) of 200,000 – estimated Re of flight experiments – MH60's stall angle is 12° and the max lift to drag ratio (L/D) angle is around 6.0° ("MH 60 10.08% (mh60-il) Polars," 2018).

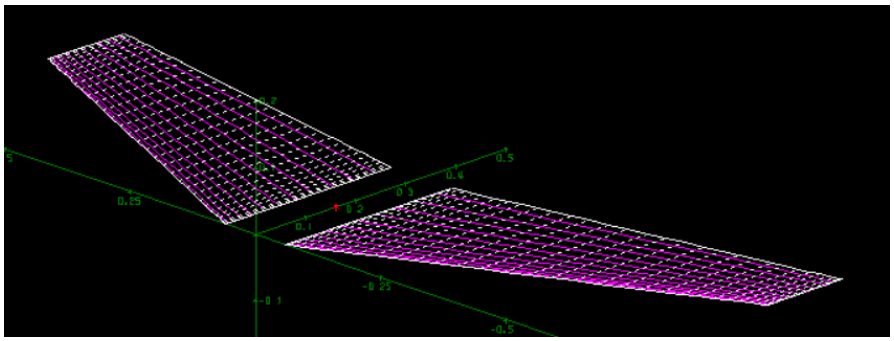

Figure 5. 3D lifting surface model in AVL

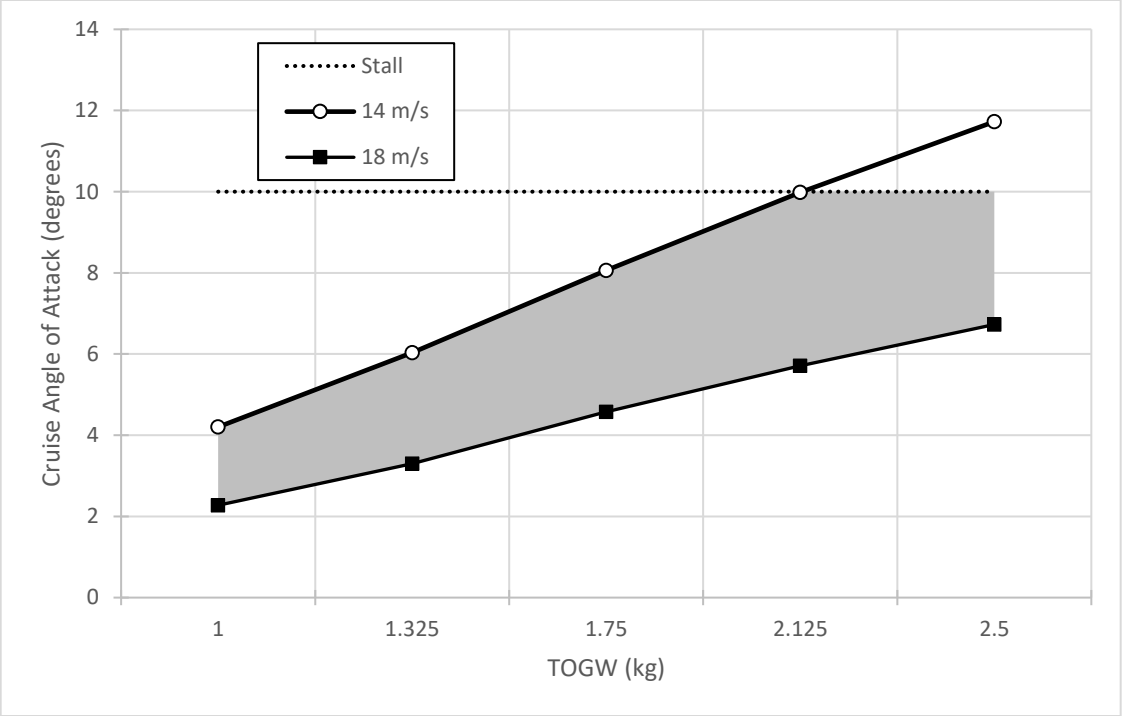

Figure 6. Trim envelope for prototype flying wings

The AVL case study on weight and angle of attack for straight and level flight led to the design point: velocity of 14 m/s, total weight of 1.5 kg, angle of attack of 6.7°. The weight was deemed obtainable from prototype builds weighing around 1.25 kg. This angle of attack is slightly above the predicted max L/D angle so that a slight loss in speed results in an increase in efficiency.

The CG was chosen experimentally and numerically validated. For a flying wing to be controllable in pitch, the aerodynamic moment should be close to zero. The desired moment coefficient is just slightly negative with a static margin around 5% (Mader & Martins). The trimmed neutral point – which is the same as the aerodynamic center for a flying wing – comes out to be 0.21 m (8.25 in) from the root leading edge. To determine the stability of the airframe, tests were made by launching controlled glider prototypes. The CG was slightly adjusted in front

of the neutral point until a pilot deemed aircraft controllable. The CG was chosen to be 7.875 in (0.2 m) which results in a static margin of 5.25%.

3.4 Avionics

Electronic components are key to making this sUAS a low-cost solution. The flight avionics were chosen based off historical use in the Unmanned Systems Lab. The battery was initially a 3S 2600 mAh LiPo but build refinement allowed for a heavier 3S 5200mAh LiPo. The motor system consists of a brushless 1300kv motor, a 9x5 propeller and a 30A electronic speed controller. The camera system is a Raspberry Pi Zero along with a V2 Camera Module. Free, simple, and open-source flight software Arduplane has been used with various compatible flight controllers. The ground station is also free open-source software, called Mission Planner (Oborne, 2016). As shown in Table 3, the estimated cost of electronics and mechanical systems adds up to $247.81. Figure (7) shows the latest layout along with a schematic of the electronics associations.

Table 3. Electronic package cost estimate

Item	Cost	Quantity	Item total cost:
30A ESC	$13.30	1	$13.30
Airspeed Sensor + Pitot Tube	$22.57	1	$22.57
3S 5200 mAh Battery	$26.45	1	$26.45
Flight Controller + Power Module	$64.00	1	$64.00
Control Horns (10pc)	$1.10	1	$1.10
Radio	$26.95	1	$26.95
Linkage Stoppers (10 pc)	$1.29	1	$1.29
Servos	$5.73	2	$11.46
Props	$2.85	6	$0.48
Motor	$16.95	1	$16.95
Flight Controller GPS	$19.99	1	$19.99
Pi zero board	$5.00	1	$5.00
Pi camera cable	$5.95	1	$5.95
Pi camera	$29.95	1	$29.95
		Total:	$247.81

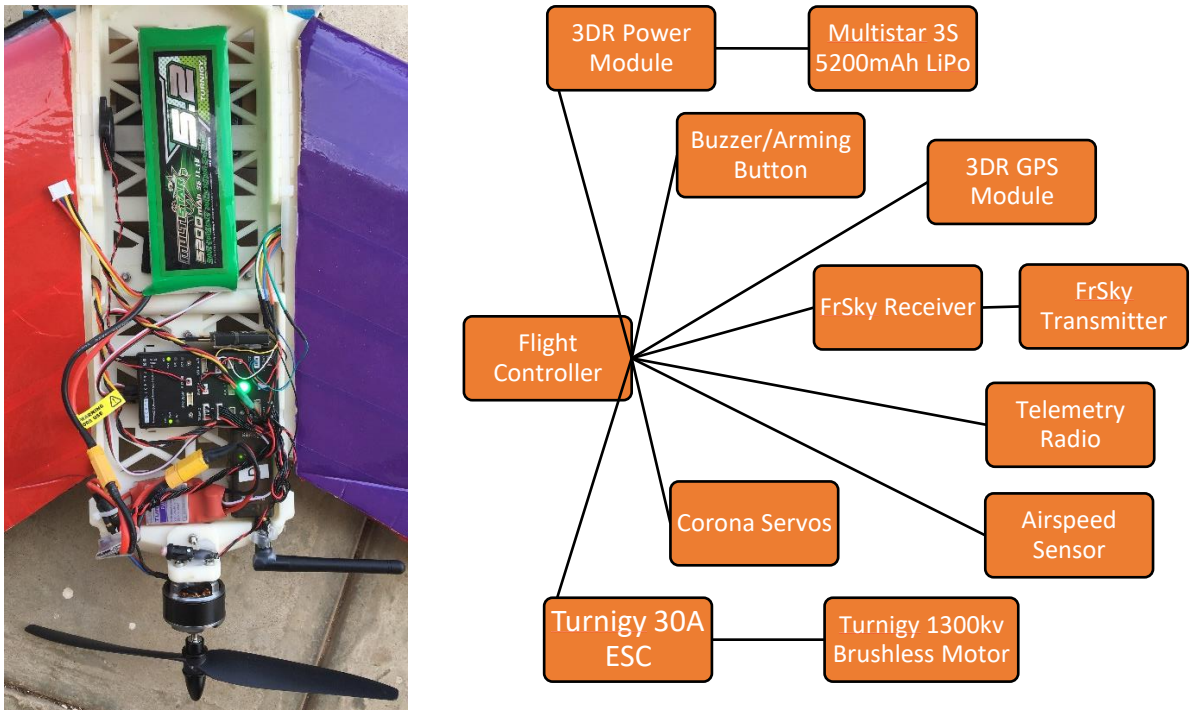

Figure 7. Layout of EcoSoar electronics

3.5 Motivation for 3D Printed Parts

Additive manufacturing presents an opportunity for production capabilities in regions where manufacturing facilities are scarce or even nonexistent. If an electronics package could be sent to the community where the sUAS is to be used, local workers could locate or print everything else needed to build aircraft. Design changes do not hinder production either; all that is needed is simple switch of the generic 3D mesh (.STL) file for the upgraded component. In addition, the aerodynamics of the system benefit from being able to produce accurate airfoil shapes with rib components. Table 4 shows the cost estimate for the structural components in a single airframe.

Table 4. Structure cost estimate

Item	Cost
PLA needed for full set of 3D Printed Parts	$12.50
Main Spar: 8 mm OD x 6.5 mm ID x 1 m carbon tube	$9.80
Leading Edge Spar: 4 mm x 1 m solid carbon rod	$5.35
Total:	$27.65

3.6 Coroplast Prototyping

An unmanned aircraft made from Coroplast was the first successful aircraft. The material is a trademarked corrugated plastic as shown in Figure (8). The initial interest in using this material to make aircraft wings comes from colleagues abroad being able to find the material in the World Bank designated low-income country, Afghanistan. Coroplast was also appealing due to it being waterproof and because the closed sections of the flutes offer lateral stiffness and axial strength. It also easily bonds to itself as well as the 3D-printer material, PLA plastic, with CA glues.

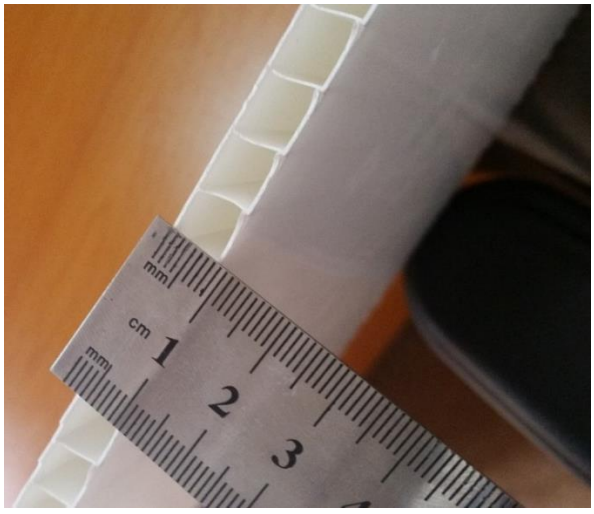

Figure 8. Close up view of flutes in 8mm Coroplast

Coroplast wing crafting techniques, highlighted in Figure (9), were developed by making glider prototypes. By removing sections from certain flutes, the Coroplast sheets could be made to bend in such a way to resemble a cambered wing. The structure of the wing was made by

gluing 3D-printed ribs integrated with a carbon fiber and foam spars onto the plastic sheets. Control surfaces were made with Coroplast sheets cut in a way that allows deflection.

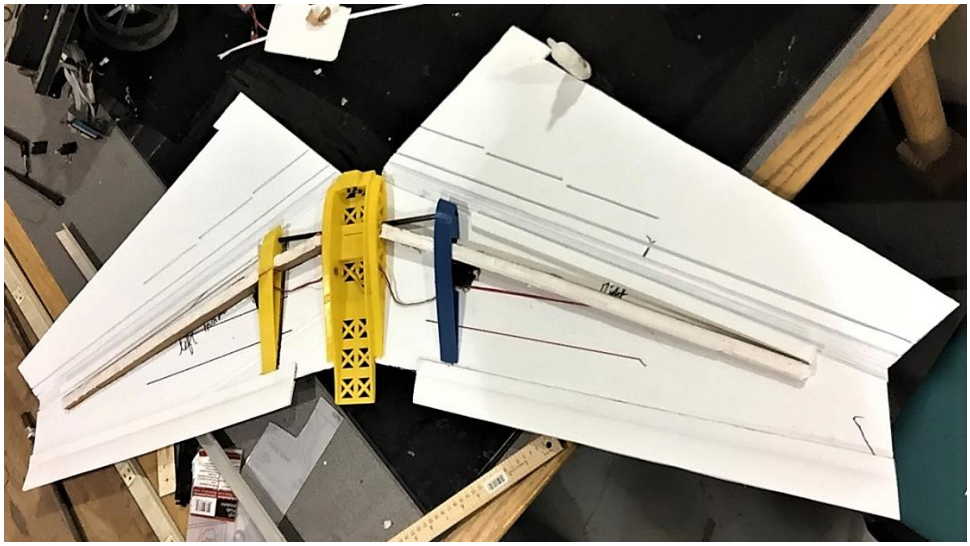

Figure 9. A look inside of the Coroplast bird, showing off the flutes cut in order to shape the wing

The resulting build was the first experimental aircraft to successfully take to the skies. The empty weight, airframe and all electronics, came out higher than wanted at 1.52 kg. Coroplast might be a viable option at another scale but this heavy aircraft could not handle a payload making it useless for imaging and delivery applications. For this reason, Coroplast was ultimately ruled out as a material option. However, and this will be expanded on later, this build proved extremely beneficial to developing launch and landing tactics due to its durability.

Chaper 4. Foamboard Prototyping

Foamboard was selected as the wing material since the resulting wings were over 13% lighter than the Coroplast counterparts were. The wings are created using a combination of foamboard, 3D printed parts, and hot glue. The first foam prototypes, nicknamed the “Foamies,” were used to test crafting techniques, imaging systems, and launch systems. Once the wing manufacturing process was solidified, aircraft “EcoBlack” and “EcoWhite” were made and used

to test autonomy. The first build to earn the title of *EcoSoar* was made with airframe upgrades determined necessary by autonomous flight experiments. Two more *EcoSoar* builds were made to test flight performance and build consistency. Noticeably, the design process was incredibly iterative but rapid prototyping proved to be crucial in order to develop crafting techniques necessary to build successful low-cost aircraft. Table 5 summarizes the design process by showing contributions of all major aircraft leading up to *EcoSoar*.

Table 5. Layout of flying wing builds which had major roles in design process

Build No.	Fuselage Version	Name	Flights	Major Contributions
1	V03	Coroplast – “Coro”	10	• First flight • Launch techniques
2	V05	Foamie – "Red"	3	• Launch tests • Stability tests
5	V05	Foamie – "Green"	6	• Imaging tests • First autotune process • First autonomous flight
6	V07	EcoBlack	16	• Confirmed PID gains transfer • Autonomous landing tests
7	V07	EcoWhite	23	• Autonomous launching tests • Autonomous flight performance evaluation • Payload bay analysis
8	V08	EcoSoar – EcoUV	5	• Motor configuration tests • Wingtip device experiments • Path following parameter analysis
9	V09	EcoSoar – EcoIR	15	• Glide ratio tests • Mission programming experiments • Complete autonomous performance evaluation
10	V10	EcoSoar – EcoSun	1	• Confirmed EcoSoar consistency

4.1 Wing Development

The Foamie builds were the first prototypes with wings made of posterboard. They were predominantly used to practice posterboard manipulation techniques such as where to remove paper, where to sand foam, how to create strong hinge lines, and how much hot glue is

necessary. All of the techniques were developed with the goal of creating an aerodynamic and lightweight structure. The wings of builds 2 – 5 utilized two carbon spars, one max thickness foam spar, a foam leading edge support along a percentage of the span, and a servo placed such that it is sandwiched by the wing when closed. The first Foamie, "Red," was shaped using foam ribs and a foam bridge as shown in Figure (10).

Figure 10. Inside look of "Red," showing the crafting techniques used to shape the wing

The paper is removed in areas to allow for curvature and glue attachment. Which allows the wing to have camber and better adhere to itself. There were several issues with this build: the leading edge gave too easily, spars did not have enough contact with the top of the wing, the end of the wings creased due to bending stress, and the servo arms were damaged on landing because they go through the bottom of the wing. The most successful Foamie, "Green," remedies these issues by prioritizing load transfer to the spars and rotating the servos. As shown in Figure (11), the foam leading edge support stiffens the nose while also connecting the spars to the top of the wing. Additionally, the foam spar resists bending at the wing tips by spanning the entire wing.

Figure 11. Inside look of incomplete "Green" Foamie, showing the elevated leading edge support used to shape the wing

Note this picture is an incomplete version of "Green." Paper must still be removed and sanded in certain areas, and the servo must be attached.

The basic idea of using leading edge support along with foam spars to transfer loads to the carbon spar is used in all future builds. The success of "Green" inspired the creation of a wing template. To keep wings constant across builds, construction lines were added to a 2D wing template to define curvature areas, part placement, and attachment areas. Drawings similar to Figure (1) were programmed into a CNC router to make wooden wing stencils. EcoBlack and EcoWhite were made using these templates and both flew tremendously. Further refinement of the wings consistency was made by replacing the foam leading edge support with 3D printed parts. To align the new components, a leading edge spar replaced the front spar of previous builds. These changes are showcased in Figure (12).

Figure 12. Insides of EcoUV's right wing, showing the new 3D printed components

4.2 Fuselage Modeling

The repeatability of wing creation definitely improved over time but the fuselage has transformed the most. Different fuselages were made to either fix an issue or test a new configuration. There are 10 different versions of fuselage, some are vastly different and others only have minute changes. Initial fuselages were too heavy or attempted incorporate infeasible wing characteristics. For example, dihedral wings were ruled out due to the inability to create a strong enough connection within the fuselage given the material restraints. The fuselages were modeled to fit electronics mentioned in Table 3, allow for a controllable weight distribution, and include provisions for a payload bay. Four fuselage designs from prototype aircraft mentioned above in Table 5 are shown in Figures (13 - 16).

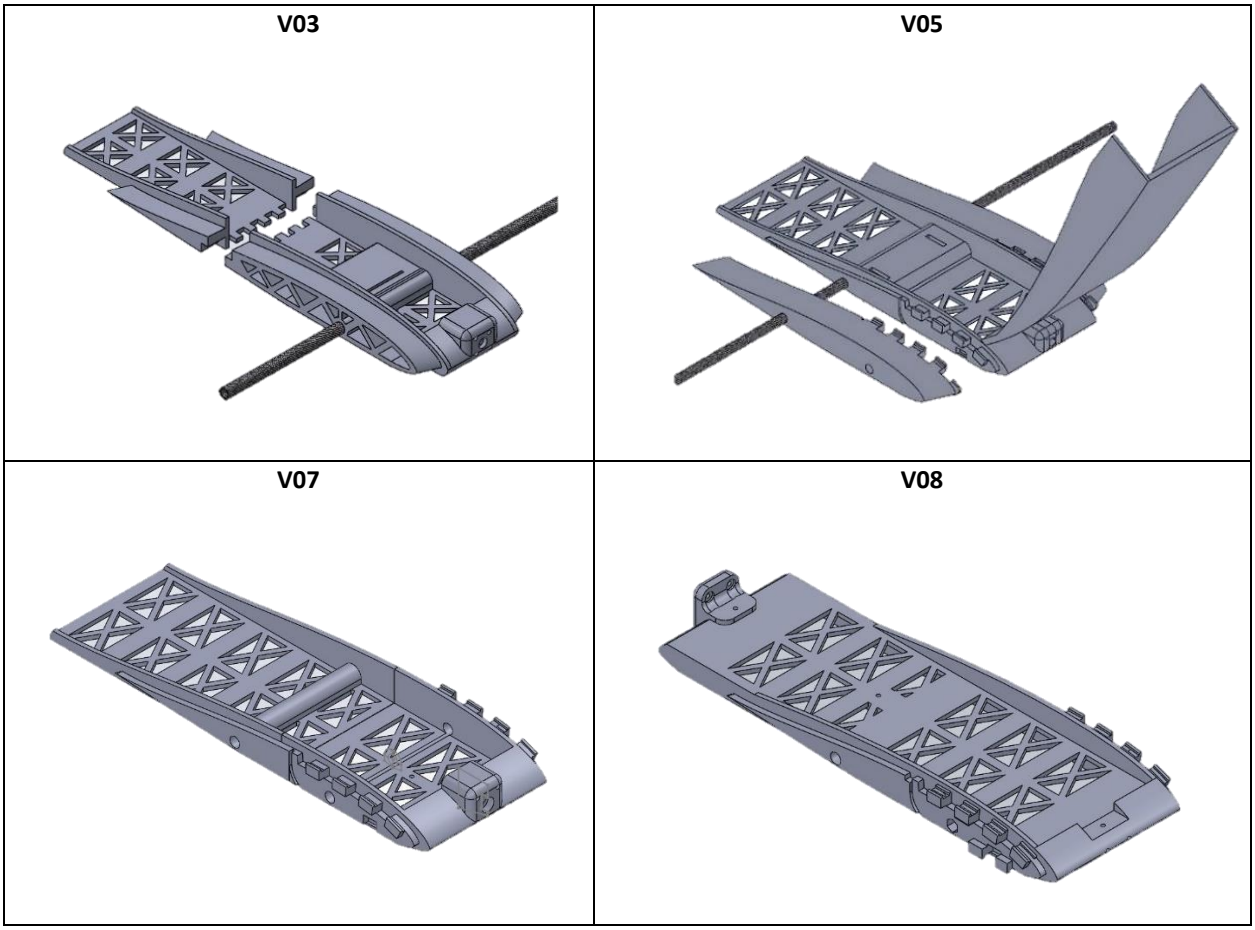

Figures 13, 14, 15 and 16. Fuselage designs of some of the foam prototypes

Though the Coroplast aircraft flew well, the fuselage did not have enough room for battery movement. Since the battery is the heaviest component of the aircraft, being able to adjust its position within the fuselage allows operators to control the CG. Every fuselage after V03 has over a 3¾" wide electronics area to allow the flight controller to rest sideways and therefore create room for battery movement. A modular wing root with a MH 60 airfoil profile was introduced in V05. The wing root is a rib that allows the wing to be independent of the fuselage. The wing and fuselage fit together by means of an original interlocking design that clamp together with a cable tie. Throughout the models above, this connection gained additional

teeth and groves for cable tie snugness. The payload bay in V05 housed the Raspberry Pi camera system, but ended up being bulky and interfering with main electronics. V07 and on allow for a modular payload bay with a connection point underneath the fuselage at the CG.

The motor mount was initially in the front of the fuselage considering safety of the hand launched system. Once launch practices improved, it was desired to move the motor to the rear in order to save props. V08 utilizes a modular motor mount, resulting in an airframe capable of both pusher and tractor configurations. To maintain CG location, the electronics bay was made to be completely flat allowing the avionics to adapt with the configuration. Other minute changes dealt with organization of wires and electronics.

4.3 Launching Systems

Proper flight behavior analysis of the foam prototypes can only occur if they first get off the ground. Developing a dependable launch system has been one of the greatest challenges. The stability threshold of a flying wing creates many issues especially when trying to launch in high winds. Tuning the initial pitch, acceleration, and final velocity of the launch has led to many solutions; from skilled hand tosses, to atlatl pole launches, and finally to bungee high starts. Even when the launches had a 90% success rate, a completely new set of problems opened up when attempting autonomous launches.

Looking back to Table 5, builds three and four are left out because they did not last long enough to contribute. This is because first flight tests were all hand launched. Discus, forward overhand, and even backwards overhead tosses were attempted. Though some flights were successful, a more reliable launching method was urgently needed to get flight data. The first solution, used on almost every Foamie flight, was a pole launching system. Contact points added

to the underbelly of the fuselage would fit into a grove on the top of pole and would only release when vertical. This allowed someone to throw the aircrafts at a higher altitude with more force.

Figure 17. Pole launching practice, using the "Red" Foamie as a glider

This method of launching was several times more reliable than hand launches, but it included too many human factors to be a long-term solution. The business model for aircraft operation requires as little training as possible. A successful – and hands-free – launching system must store energy, then release the aircraft at a reasonable airspeed and pitch angle. This logic led to the next system, which is popular in the hobbyist community, a bungee launch. The bungee used is 25 ft of thick synthetic latex tubing that can stretch up to four times its length, maxing out with a compression force of 15 lbs. The basic idea of this system is to pull the aircraft in such a way it gains altitude and releases when the bungee slides off a hook attached to the fuselage.

The challenge of creating a bungee launching system is deciding where to pull the aircraft. If pulled from the nose, the aircraft would fly straight to where the bungee is anchored. If pulled from the CG, the aircraft would freely pivot on the attachment point and crash. The aircraft must be pulled somewhere between these two locations to cause a small positive pitching

moment, resulting in brief ascension like a kite catching air. This gain in altitude allows safe acceleration to cruise airspeed. The aircraft is released when the hook passes over the bungee anchor. An action photo is shown in Figure (18) to show the altitude gain.

Figure 18. Bungee launch from the view of the anchor point

The anchor point can be anything that can withstand 15 lbs, ground stakes, tables and even vehicles have been used. The foam prototypes used in the first bungee launches tested several types of hooks and hook locations. These connection points varied from angled nails to 3D printed hooks. The location of the tension point was narrowed down by gradually increasing the distance between it and the CG. Small distances caused too much pitch and resulted in the aircraft rolling back toward the ground due to tip stall. Launching into winds above 7 mph also caused this tip stall issue because the aircraft would catch too much air at the beginning of the launch. It was found that aircraft had to remain under 35° of pitch in order to retain control and thus roll stability. Once the launch dynamics were relatively stable, the “Green” Foamie was used to test autonomous capabilities of launch.

Ardupilot checks for a minimum airspeed and acceleration before initializing a countdown to powering the motor. These were easy to calibrate using data from numerous launch tests where typical launches experienced up to 3 g's of acceleration and left the bungee at 18 m/s. Minimum airspeed and acceleration were programmed to be 8 m/s and 1.5 g's so that conditions are always met in launch. The countdown was set to one second to allow the aircraft to detach from the bungee rope before throttling up.

To address the issue of launching into the wind, the bungee hook was refined to have multiple tension points. As shown in Figure (19), the four rungs allow for various launch dynamics due to resulting moment. The top point is to be used for launching into the wind, as it will keep the aircraft most level. The bottom point results in the greatest pitch angle and therefore the most altitude gain. Now operators only need to pull back a bungee and choose which rung is best for takeoff; the aircraft will do the rest.

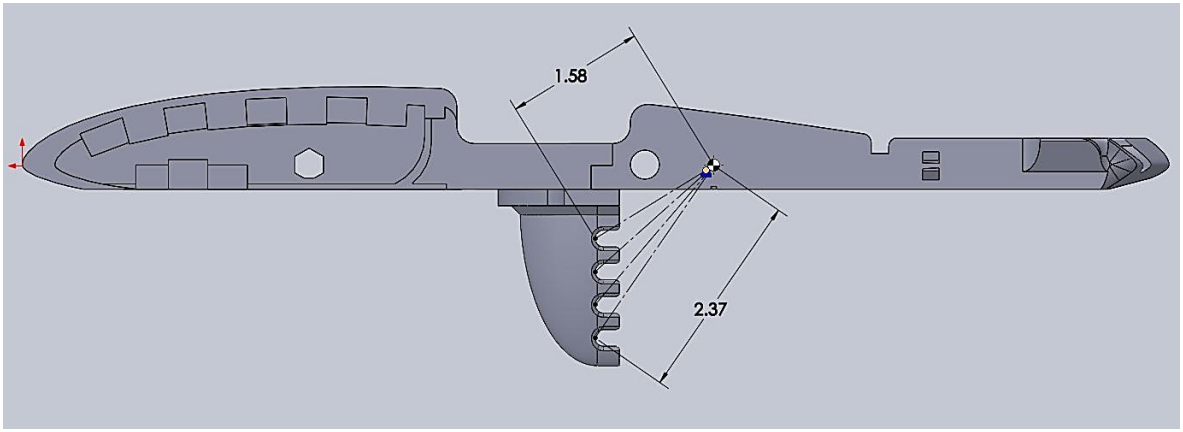

Figure 19. Aircraft bungee hook with rungs for different launch scenarios, dimensions are in inches

4.4 Wingtip Apparatus Development

Flying wing aircraft lack vertical stabilizers and have a shortage of control surfaces. Vertical surfaces behind the CG help stabilize the aircraft by resisting sideslip and forcing the nose into the flow. Aircraft typically use 4-channel control systems: ailerons, elevator, throttle,

and rudder. The rudder is not actually necessary for controlled flight, it is predominantly used for ground steering and adjusting the nose in banks. For this reason, RC-grade flying wings tend to reduce the control system to 3-channels: ailerons, throttle, and elevator. While this system is stable through controllability, the use static vertical fins behind the fuselage or side-force-generators (SFG) on the wing tips can support roll and yaw stability. The further these vertical surfaces are from the CG the larger the effect of weathervaning, which is the aircraft tendency to point into the airflow. Therefore, it was decided to add an endplate on the foam prototype wingtips.

Another wingtip configuration initially considered were winglets. Winglets can lessen the induced drag of the aircraft while still creating enough side force for directional stability. Winglets work by weakening the vortices shed at the wing tips, thus improving endurance and range of aircraft. Winglets can be quite beneficial if the reduction in induced drag overcomes the consequential parasitic drag.

4.4.1 3D Printed Winglets

Since the 3D printer allows for the most creative freedom within the scope of this project, the winglet design took a quick turn toward CAD. To have an effective winglet, the wingtip must be a lifting surface and therefore have airfoil cross sections. The highly cambered NACA 6412 airfoil was used to model a winglet for the foamboard prototypes. A winglet connection region, with a MH 60 profile like the wing root part, allows the winglet to be anchored in the wing tip. As shown in Figure (20), the airfoil loft modeled is slightly swept, extending 2.0” out and 3.5” up. Though a useful, not to mention aesthetic, solution to aid aircraft roll and yaw stability, plastic winglets are heavy and incredibly difficult to replace.

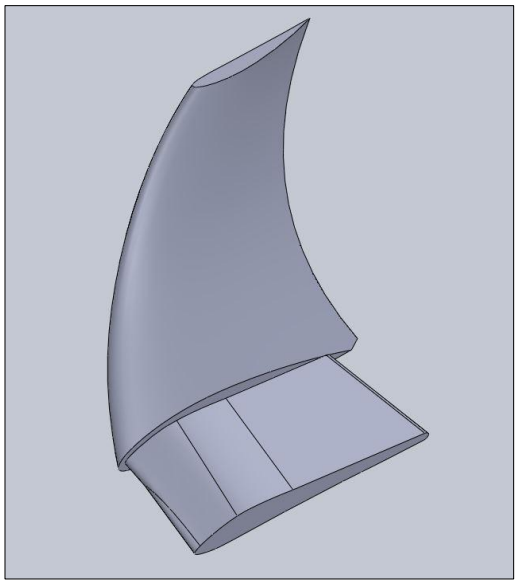

Figure 20. Basic winglet model created for foamboard prototypes

4.4.2 Foamboard Endplates

All foam prototypes made before EcoUV had 3D printed winglets. The winglets weighed between 40 – 60 g, adding up to almost 10% of the aircraft total weight. A lightweight approach to developing wingtip endplates was formed using foamboard, the same material as the wings. The foamboard can easily be cut, sanded to points, and taped to resemble practically any shape. A simple "house" shape is cut so that the new fin extends 2" below and 3" above the wing. These are then capped onto a 3D printed rib placed at the far end of the wing. The foamboard wingtip is shown in Figures (21 - 22).

Figures 21 and 22. Zoomed in photos of prototype highlighting foamboard wingtips

To validate the decision to switch wingtip devices, the two V07 birds, EcoBlack and EcoWhite, were compared with the first UAV to have foam SFG's, EcoUV. Benchmark missions were created to compare current consumption, turning radii, and climb characteristics across builds and parameter changes. It should be noted, all aircraft have the same gross weight and attitude PID gains throughout the following benchmark tests. The missions used to evaluate wingtip apparatuses are presented in chronological order by Figures (23 - 25).

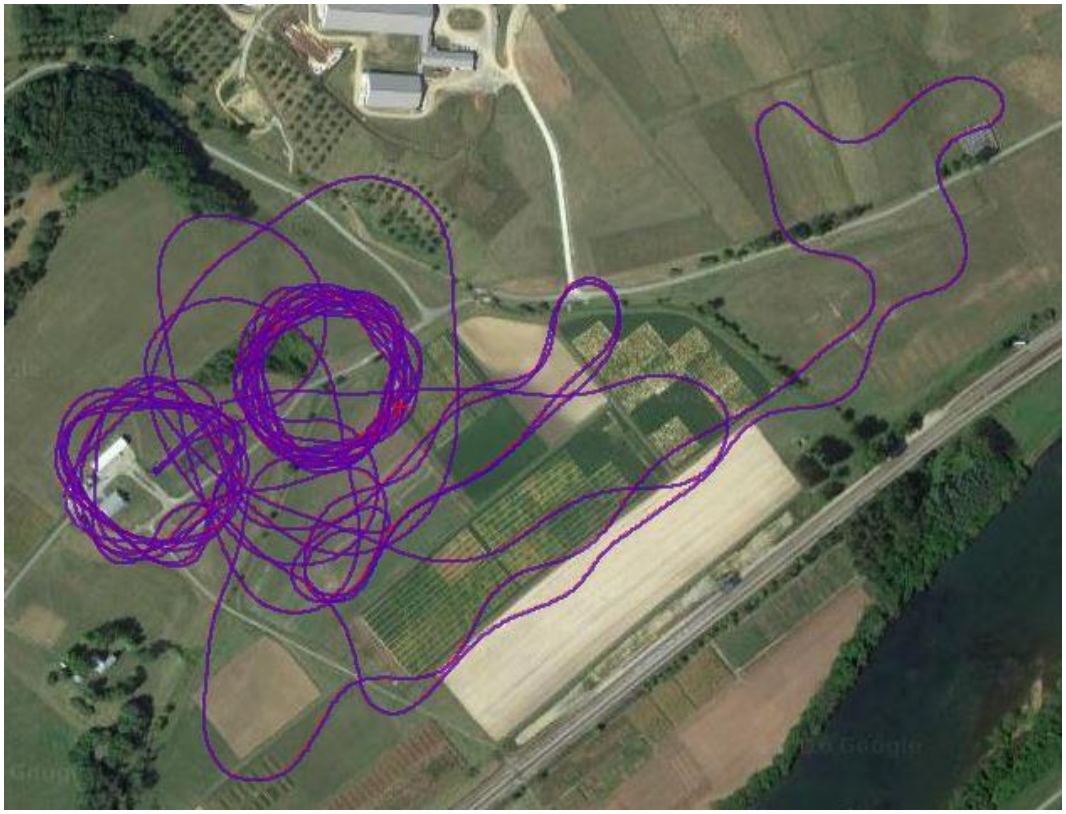

Figure 23. EcoBlack's path on its 12th flight

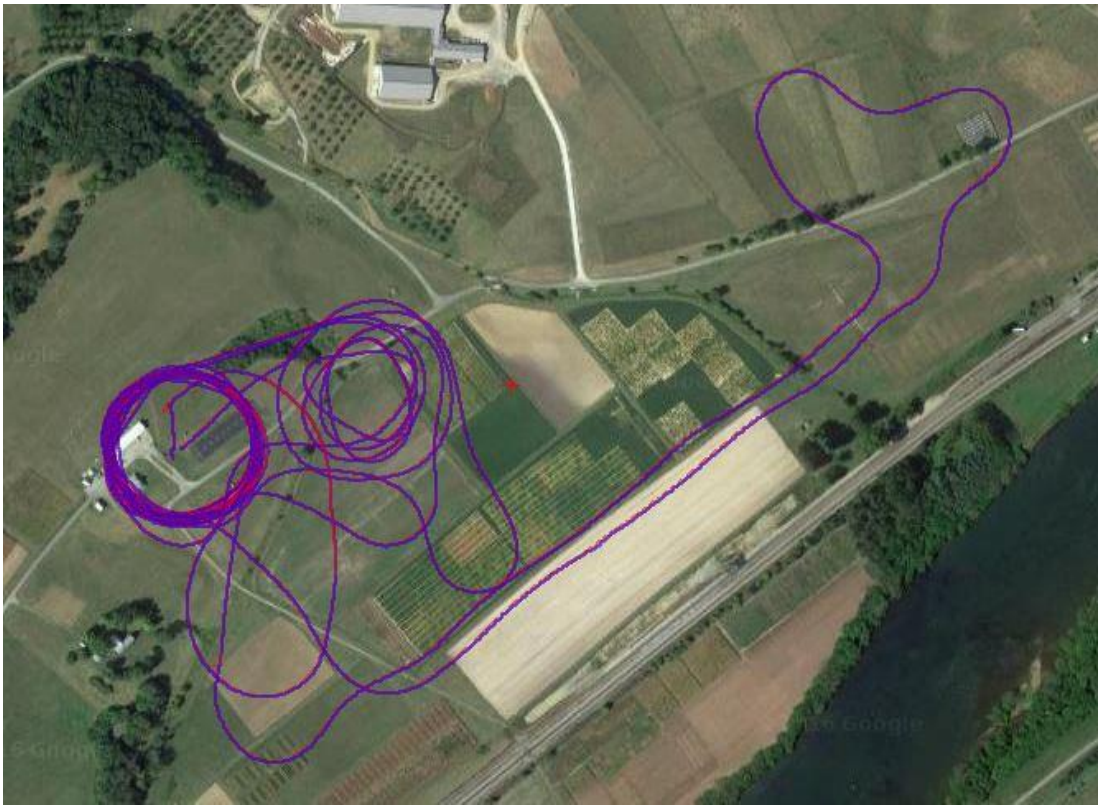

Figure 24. EcoWhite's path on its 12th flight

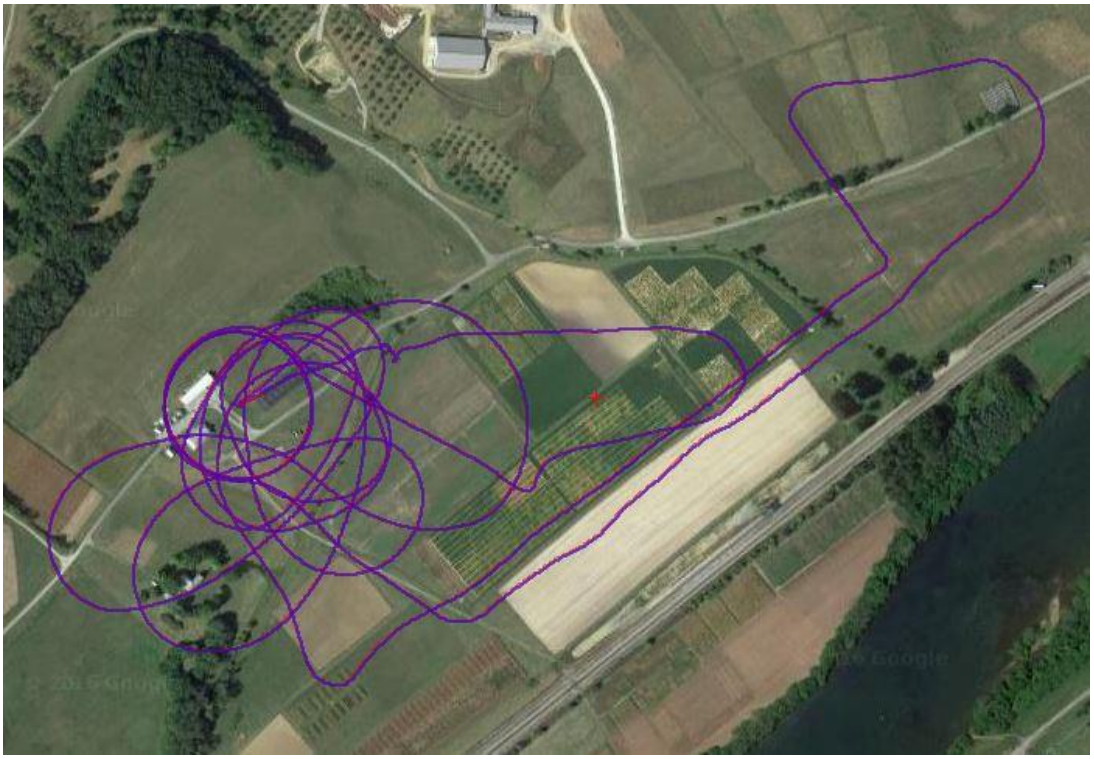

Figure 25. EcoUV's path on its very first flight

One can see obvious improvement throughout the figures above. The circle to the west gets tighter and the 0.5 km straight and level paths become increasingly linear. The snaking behavior of EcoBlack's path was a huge red flag. The path-following tuning was too aggressive, making the aircraft overshoot when attempting to navigate back to the path. The navigation tuning was relieved with a damping parameter called NAVL1_DAMPING. This was fixed before EcoWhite and EcoUV's flights so these aircraft only differed in wingtip device. Drag differences from the straight and level flight paths are inconclusive; the aircraft have too similar current draw and angle of attacks. If the winglets reduced drag, it is not enough to be noticeable. However, roll and directional stability differ between builds. Roll, pitch, altitude, and current for both aircraft were logged while in the circular loiters to assess the difference. This data is shown in Figures (26 - 27).

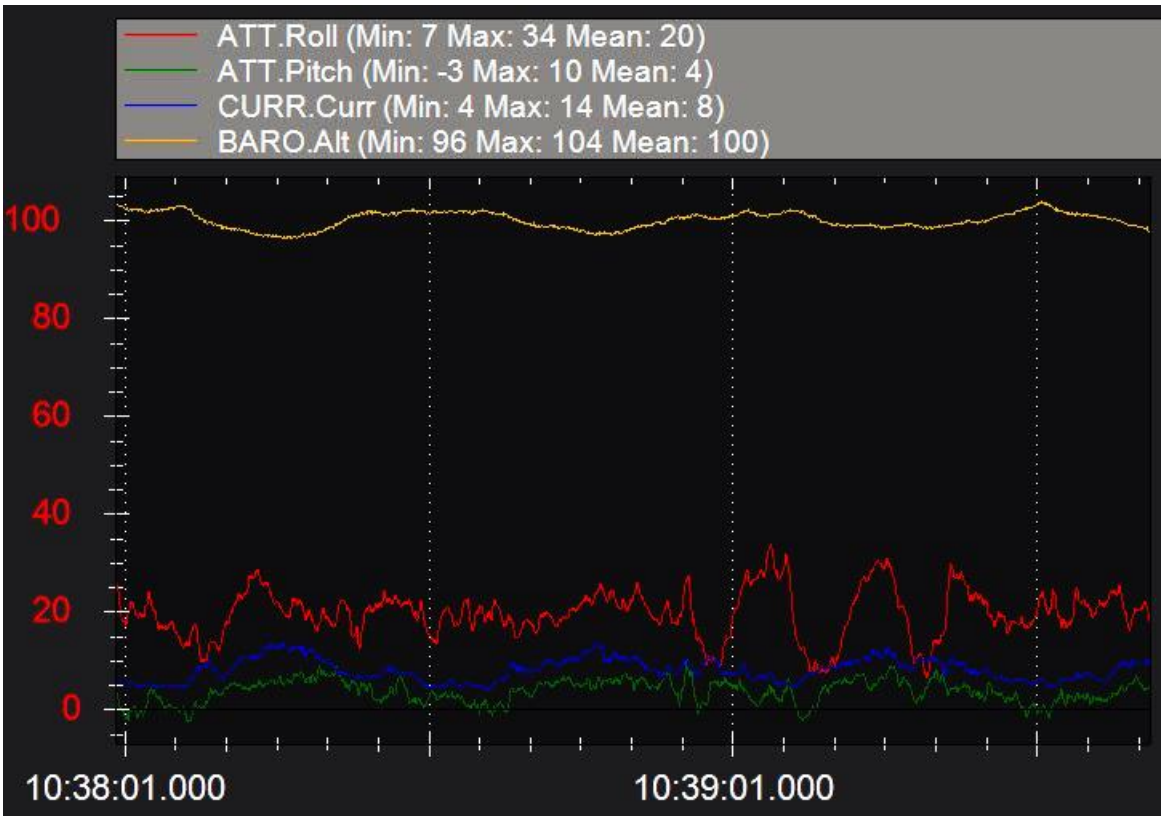

Figure 26. Pitch, roll, altitude, and current draw of EcoWhite in loiter

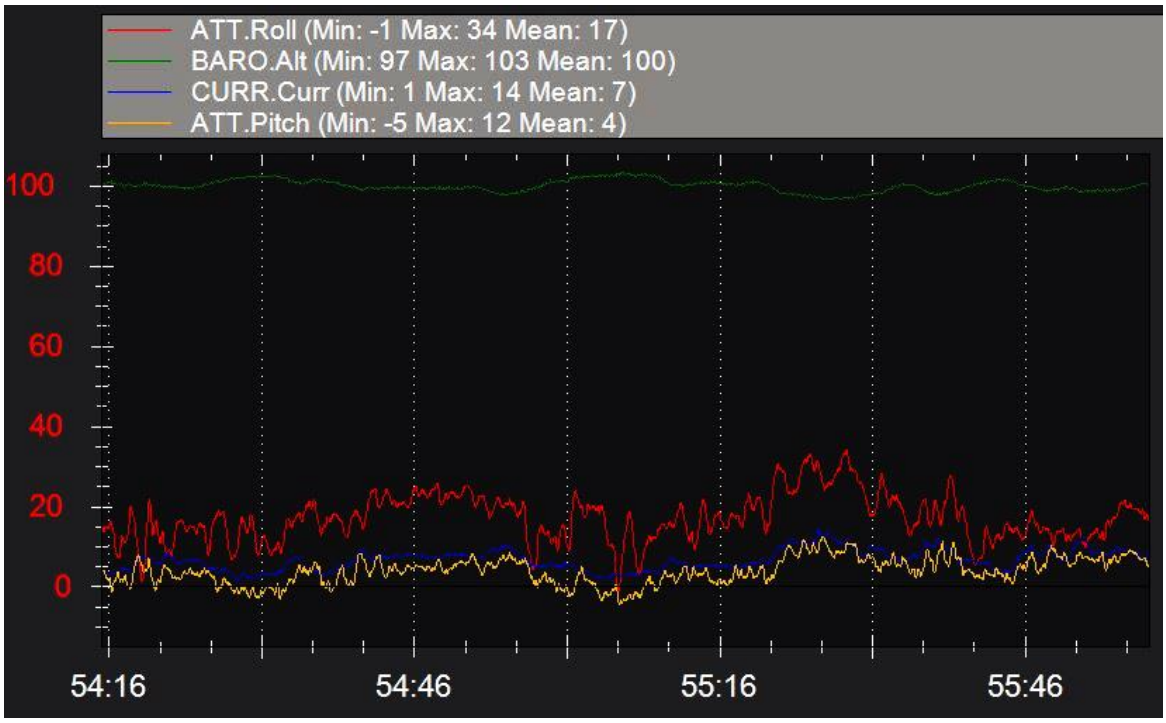

Figure 27. Pitch, roll, altitude, and current draw of EcoUV in loiter

The two data sets shown above represent how well the aircraft resist sideslip in a 90 m radius turn for about 100 s. They manage to hold altitude well, both averaging out exactly at 100 m. However, EcoWhite's deviation is ±4 m where EcoUV's is ±3 m. EcoUV also has a lower average bank angle and current draw than EcoWhite. Meaning, EcoWhite was trying harder to hold altitude while turning. The foam SFG worked as predicted by reducing the empty weight of the aircraft and increasing roll and directional stability.

4.5 Imaging

The imaging system is a modular payload consisting of a Pi Zero, a V2 camera module, and a 3D printed case that attaches to the underside of the fuselage. The camera payload is protected by the bungee hook used for launch. A python script starts the camera when power is applied. During flight, the Pi Zero records timestamps along with corresponding raw images fom the camera and GPS serial data from the flight controller. A Robotic Operating System (ROS)

based post processing procedure combines the images and GPS data by connecting timestamps. An example of the stitched imagery from an EcoSoar flight is shown in Figure (28).

Figure 28. Mosaicked images of Virginia Tech's airspace research center, Kentland Farms

Chaper 5. EcoSoar

The foam prototypes were refined flight test after flight test – build after build. This rapid prototyping approach ended after EcoUV was made. To fulfill the requirements of production and operation needs, EcoIR and EcoSun were made within the scope of the business case. The total aircraft cost is around $275, as reflected by Tables 3 and 4, and is subject to change due to fluctuations in individual components market prices. Crafting techniques were replaced by strict part placement and manufacturing instructions. Flight controller calibrations were replaced by electronic quality checks. Flight configuration experiments were replaced by autonomous performance evaluation. Every step used in the production and operation of *EcoSoar* was recorded and is laid out in this chapter. EcoIR is shown in Figure (29).

Figure 29. EcoIR, the first EcoSoar model to not need any tuning

5.1 Airframe Layout

EcoSoar's airframe combines 3D printing technologies with low-cost posterboard. Spars in each wing thread through the fuselage, airfoil shaped ribs, and leading edge supports. The main spar is detachable, allowing for modular wings. The leading edge spar is cemented in each wing to ensure part alignment. The leading edge supports are lightweight and prevent nose deformation. The ribs house the servomechanisms used to actuate the control surfaces. This forces the control mechanisms to the same location throughout builds. The layout is as shown in the transparent body of Figure (30).

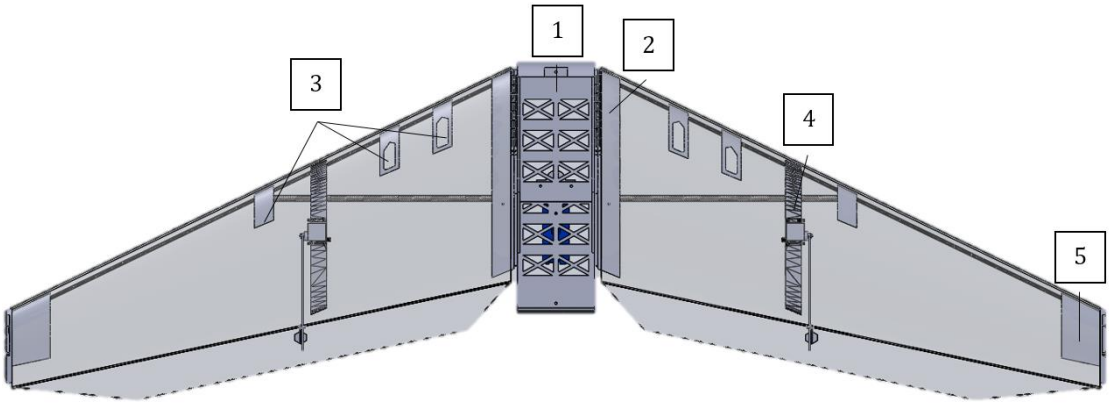

Figure 30. Solidworks model of EcoSoar highlighting 3D printed compoenents

1. Fuselage
2. Wing Root
3. Leading Edge Support and Spar Joint
4. Servo Rib
5. Wingtip Mount

5.2 Production

The manufacturing process should be rapid, ensure replicability, and take place within the community of operation. The goal of EcoSoar production is to reduce time and skill required. Guides and tools have been made to aid in the consistency across builds.

5.2.1 Template

A wing template, as shown in Figure 31), has been made with ¼” wood on a CNC router to help create the wings. The template comes from the wing drawing in Figure (1), with additional markings used to make the foam spars. The shape is exactly 30” x 20” in order to fit over a piece of posterboard. A pencil or paint can be used to transfer the markings onto the posterboard like a stencil. The markings show details such as where to cut the foam, where to cut the paper, where to place parts, and where glue attachment areas are.

Figure 31. EcoSoar wing template

5.2.2 Instructions

A document along with a video series, the latest can be found here, has been prepared for manufacturing instructions. These were tested in a workshop where 13 students with no related backgrounds made five aircraft. Shortcomings of this experience led to refinement of production documentation. Figures (32) and (33) show the finished wings just before they are closed. A summary of the instructions is given here:

- Introduction
    - Quick intro to EcoSoar and how wing shape is important for performance
- Basic Skills Required
    - Defines utility knife cuts to be used: through cut, 1% cut, and 90% cut.
    - Hot glue gun consistency is needed
- Getting Started
    - Introduction to the template
    - Where the through cuts are for foam removal
    - Where the 1% cuts are for paper removal, this is where the foam needs curvature or to be glued
    - Where the 90% cuts are for hinge lines, this in where the control surface is
    - Where 3D parts need to be placed
    - Taping the outside of the foam for friction reduction and water resistance
- Control Surface – Part I
    - Creating the hinge line with 90% cuts and sanding down foam

    - Strengthening the hinge line with hot glue
- Part Assembly & Placement
    - Right wings get a GPS, servo rib shows where to place
    - Left wings get a pitot probe on the wingtip, airspeed sensor is to be placed with in the wing
    - 3D printed parts align with spars such that placement should be easy
    - Foam spar created from other markings on template, these run down the max thickness line of the wing
    - Servos must match the correct servo rib and arm must be zeroed perpendicular to bottom side of foam
- Closing the Wings
    - Sand down trailing edge of wing (not control surface) to reduce thickness
    - Glue down wires at wingroot and along wire chase to prevent wires getting stuck or unplugged within the wing
    - Create hole for servo arm to poke through top of wing
    - Closing the wings requires quick gluing and consitent pressure, sandbag or 3 sets of hands are advised
- Control Surface – Part II
    - Servo horn placement also in template
    - Control rod z-bent on servo side, control linkages used on control horn side
    - Control surface zeroed to be in line with bottom of the wing, this can be done on any flat surface

Figure 32. Inside look of EcoIR's right wing

Figure 33. Inside look of EcoIR's left wing

5.2.3 Fuselage

The fuselage is the main component that defines an aircraft's functionality. It houses electronics, payloads, ties the airframe together, and in the case of EcoSoar, it helps the DIY part of the production process. Guides lines show exactly where the flight controller should be; other components have less strict locations. The area for the battery is large enough to correct problems with the weight distribution. The cable tie connection and rear wingroot notch force the wings to align while also adding support. The motor mount is modular, allowing for changes future configuration changes like thrust angle. The nose is flat so simple posterboard covers can wrap around electronics and payloads. Figures (34) and (35) show the fuselage CAD model and printed components ready-to-fly.

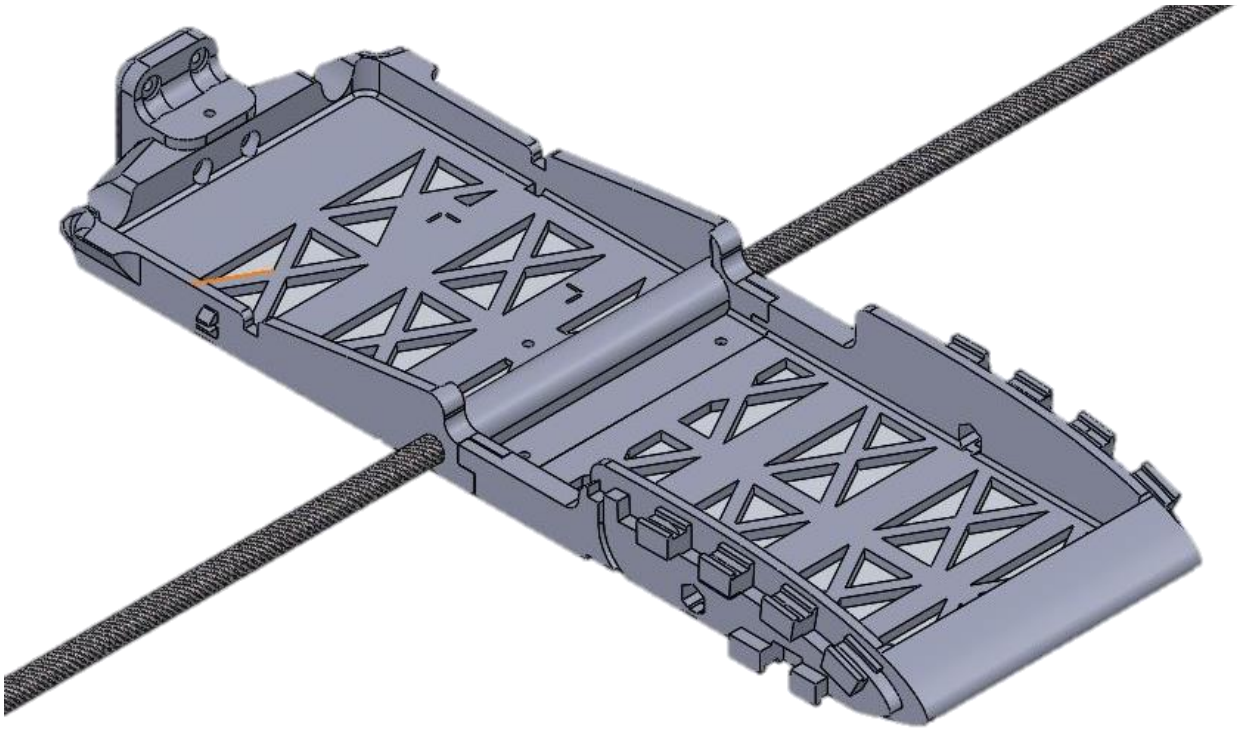

Figure 34. V10, the fuselage model used by *EcoSoar* UAV

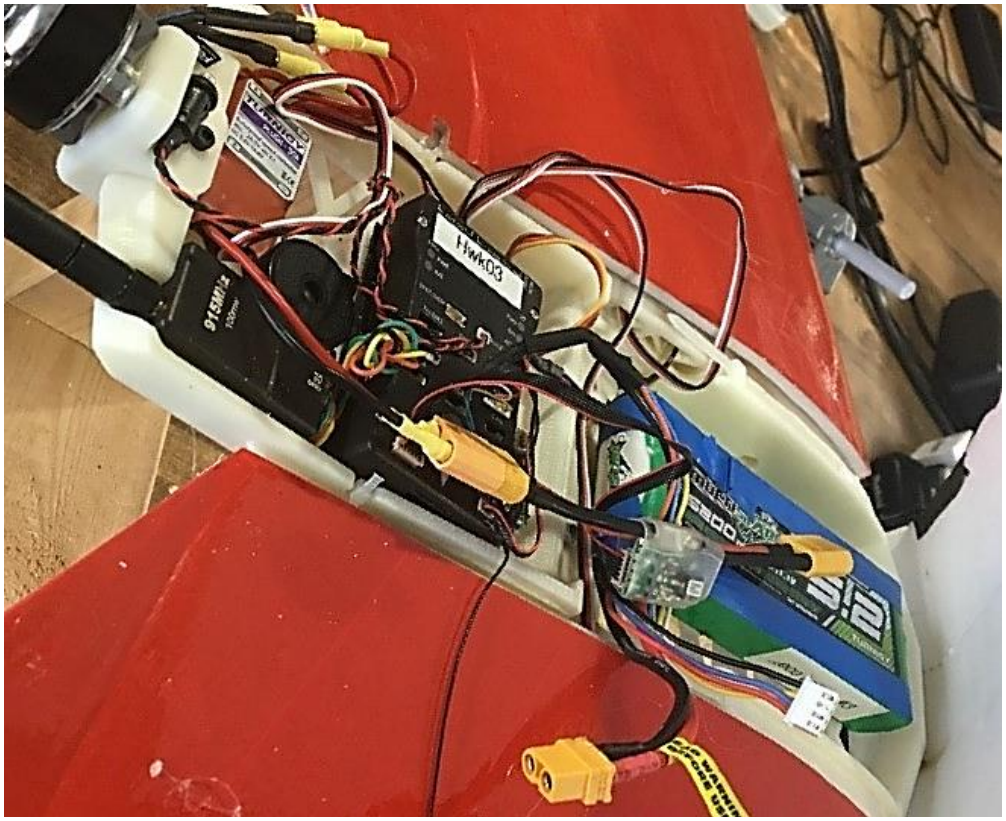

Figure 35. EcoIR with all electronics in place

5.3 Weight Summary

The weight of EcoSoar is broken down into three categories: electronic components, 3D-printed parts, and other. The avionics make up the majority of the weight because of the battery, which makes up about 22% of the total aircraft weight. The design weight of EcoSoar is 1.5 kg, so the empty weight of the airframe with all electronics drives what the payload can be. Table 6 lists every component and their individual mass, as well as the total weights of every category and resultant payload.

Table 6. Weight data for EcoSoar

Electronic Components	Weight (g)
Multistar 3S 5200mAh Battery	330
Flight Controller with Buzzer/Switch	54
Power Module	50
30A ESC	25
Reciever and GPS	37
Airspeed Sensor and Probe	12
Radio	6
Both Servos	25
Motor	75
3D Printed Components	**Weight (g)**
V10_Fuselage_Front	68
V10_Fuselage_Back	63
Wingroot_Right	55
Wingroot_Left	55
LE_Support_Right	15
LE_Support_Left	15
Spar_Joint_Right	8
Spar_Joint_Left	8
Servo_Rib_Right	32
Servo_Rib_Left	27
Wingtip_Mount_Right	17
Wingtip_Mount_Left	17
Bungee_Hook	18
Other Components	**Weight (g)**
Wings	130
Main Spar	30
Both LE Spars	20
Hot glue / tape used	45
9x5 Propeller	22
Both Control horns/rods	14
Weight Summary	**Weight (g)**
Total Weight (Avionics)	614
Total Weight (Plastic Components)	398
Total Weight (Other)	261
Empty Weight	1273
Payload (1500 -TOGW)	227

5.4 Mission Planning

EcoSoar's ground station requires a device with Mission Planner installed that either has internet connection or pre-fetched map data. Waypoints can be programmed in Mission Planner's "Flight Plan" tab, and can be sent to the UAS over telemetry or USB connection. Proper mission planning minimizes risk. Keep missions within achievable performance parameters as laid out in this section. Refer to Figure (36) for a sample mission.

Waypoints

WP Radius 20 | Loiter Radius 75 | Default Alt 60 | Relative | Verify Height | Add Below | Alt Warn 0 | Spline

	Command	Pitch/ Angl						Alt	Delete	Up	Down	Grad %	Angle	Dist	AZ
1	TAKEOFF	10	0	0	0	0	0	8	X			0.0	0.0	9174448.0	128
2	WAYPOINT	0	0	0	0	37.1944759	-80.5759192	30	X			8.1	4.7	367.1	137
3	WAYPOINT	0	0	0	0	37.1941854	-80.5713487	60	X			7.4	4.2	407.2	95
4	WAYPOINT	0	0	0	0	37.1955870	-80.5706620	60	X			0.0	0.0	167.3	21
5	WAYPOINT	0	0	0	0	37.1966467	-80.5743313	30	X			-8.7	-5.0	347.0	290
6	LAND	0	0	0	0	37.1975355	-80.5779791	0	X			-8.9	-5.1	339.2	287

Figure 36. Sample mission showing all required waypoints

5.4.1 Launch

The first waypoint of every mission is in the Mission Planner drop down menu as "TAKEOFF." This allows the motor to kick on automatically once a certain acceleration and airspeed is felt. In the Takeoff command row, change pitch angle to 10° and keep altitude low (5 m – 15 m). Once the UAV hits the target altitude it proceeds to the next waypoint. This allows your mission to have more control of the climb portion of the mission. Be conservative with the

following waypoints to aid climb to cruise altitude. From the sample mission in Figure 10, the first actual waypoint in the second row has a lower altitude for this reason. A good rule to follow is to keep climb gradient percent under 9%.

5.4.2 Fixed-Altitude Mission

Make sure to change the drop down selection next to "Default Alt" to relative. This makes waypoint altitudes relative to home rather than absolute. Cruise altitude can vary, though a good window to stay in is between 60 m to 130 m. Mission Planner estimates mission total distance in the top left corner of the Flight Plan screen. Make sure missions are no more than 25 km if using a full 3S 5200 mAh battery. EcoSoar can make tight turns. However, it is advised to keep waypoint turns above 90°.

5.4.3 Landing

The last waypoint of every mission will be "LAND." Make sure the last row's altitude column is set to "0" if landing near takeoff point or defined such that the relative altitude matches the GPS altitude in the elevation graph. To navigate to the elevation graph, right click on the map, click Map Tools, and select Elevation Graph. A path of waypoints with decreasing altitudes before the landing (keeping decent gradient less than 12%) can help avoid obstacles in the area. An example of a mission landing at a different altitude than launch is shown below.

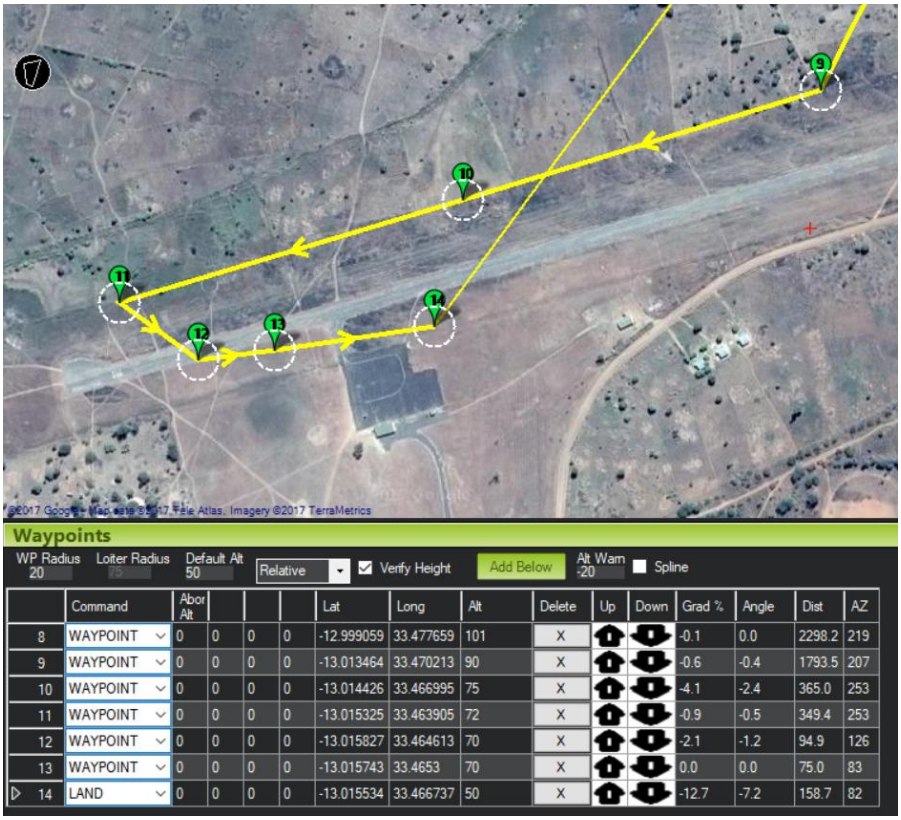

Waypoints

WP Radius 20 | Loiter Radius 75 | Default Alt 50 | Relative | Verify Height | Add Below | Alt Warn -20 | Spline

	Command	Abor Alt				Lat	Long	Alt	Delete	Up	Down	Grad %	Angle	Dist	AZ
8	WAYPOINT	0	0	0	0	-12.999059	33.477659	101	X			-0.1	0.0	2298.2	219
9	WAYPOINT	0	0	0	0	-13.013464	33.470213	90	X			-0.6	-0.4	1793.5	207
10	WAYPOINT	0	0	0	0	-13.014426	33.466995	75	X			-4.1	-2.4	365.0	253
11	WAYPOINT	0	0	0	0	-13.015325	33.463905	72	X			-0.9	-0.5	349.4	253
12	WAYPOINT	0	0	0	0	-13.015827	33.464613	70	X			-2.1	-1.2	94.9	126
13	WAYPOINT	0	0	0	0	-13.015743	33.4653	70	X			0.0	0.0	75.0	83
▷ 14	LAND	0	0	0	0	-13.015534	33.466737	50	X			-12.7	-7.2	158.7	82

Figure 37. Screen capture of Mission Planner's Flight Plan screen showing landing waypoints

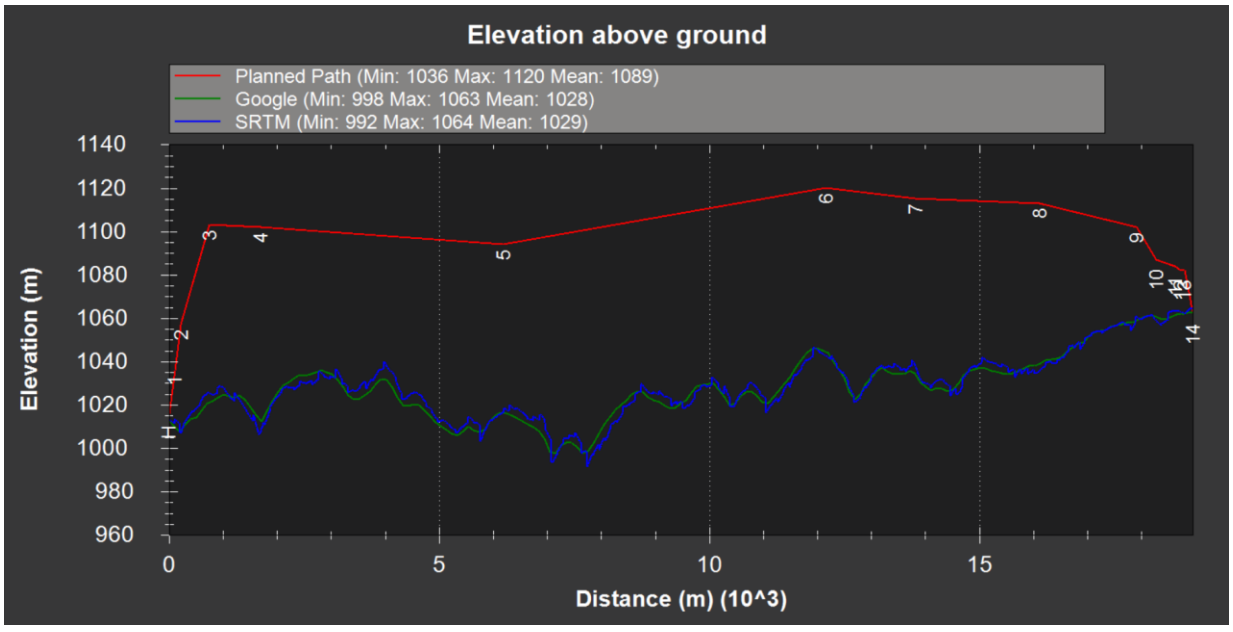

Figure 38. Elevation graph provided by Mission Planner showing relative altitude vs ground altitude

Notice how the landing altitude is 50 m instead of 0 m. The elevation graph shows the flight path over satellite altitude data, and the two lines connect at the landing waypoint.

5.5 Flight Operations

5.5.1 PreFlight

As a DIY aircraft, EcoSoar is prone to damages. Careful inspection before and after flights can help ensure safe and successful flights. Quality checks have been developed for EcoSoar for this reason. Table 7 shows the respective checklist used before every mission.

Table 7. Preflight checklist for EcoSoar Missions

Ready to Fly Checklist		
	Control Surfaces	No bends in control rod
		Control horn secure
		No twist/flex in control surface
	Motor	Shaft is tight, check set screws
		Bell is secure, does no lift from coils
		Current check at full throttle, ~25A
	Wiring	Motor spins right direction, swap two motor > ESC wires if necessary
		Motor > ESC > PM > Flight controller
		Pitot > Flight controller
		Servos > Flight controller (left wing ch. 1, right wing ch. 2)
	Airspeed Sensor	Probe is clean and well-connected, loose pitot could affect airspeed data
	Radio	Transmitter is charged and connected to onboard radio
	Controls	Manual control surface check
		FBW control surface check
	Camera	Check wiring and connections
		Pi SD card completely empty
		Plug into Telem2
Preflight Checklist		
	Weather	Ample amount of daytime left, no night flying
		Wind speeds lower than 11mph (18km/h)
	Pre-arm	GPS lock ok, (6+ sats)
		No compass variance error, compass calibration if necessary
		SD card has ample room ("Bad Terrain Data" or "Logging Fail" errors)
		Bungee force ~12 lb
		PREFLIGHT CALIBRATION for airspeed sensor, blow to ensure functional
	Mission Planning	Boxes relative and verify height are checked
		Cruise speed 14m/s
		Takeoff command, pitch 10 degrees, alt >10m
		Landing altitude checked on elevation graph
		All climb angles in Mission are less than 9degrees
		All descent rates are less than 12degrees
	Misc.	Flight mode: auto
		Make sure video is recording if needed
		Battery charged and strapped in

5.5.2 Launch

The launching system must first be setup. The anchor is to be grounded around 90 ft from launch location, use a fish scale to ensure force is 12.5 lb. If ramp is used it should be secured to the ground and level. Do not stretch the bungee for extended periods or allow it to get hot because it will lose some strength. Before launching the UAS, be sure to have telemetry connection so in-flight data can be seen and recorded. Ardupilot systems record two types of logs for flight data, flash logs onboard the flight controller and telemetry logs through the ground station. The Raspberry Pi should be plugged into the Telem2 port of the flight controller at this point. Perform an airspeed calibration by selecting the "PREFLIGHT_CALIBRATION" on the Mission Planner Flight Data tab, then clicking "Do Action" while the aircraft pitot probe is covered. Once this is done, noise from the airspeed sensor should lessen. It is normal to see a static airspeed sensor read 0.0 – 2.0 m/s. It will be more accurate in flight.

Figure 39. Actions screen of the Mission Planner GUI

Once ready for launch, choose a bungee hook rung. There are four rungs. The rungs closer to the fuselage keep EcoSoar more level during launch, and should be used in higher wind conditions. The rungs further from the fuselage allow more pitch and therefore altitude gain. If videos are necessary for mission, make sure cameras are on. Finally, switch the flight mode of EcoSoar to "Auto." This is done by either flipping a preprogrammed switch on the transmitter or through the ground station on Mission Planner's Actions tab as shown in Figure (39).

5.5.3 During Flight

It is important to watch the voltage and current draw of the UAS in flight. Normal cruise current is between 3 – 8 A. If the voltage drops below 9.9 V then it is advised to perform an emergency landing. This can be done with a pilot or an RTL command followed by a landing mission upload. Suggestions for Mission Planner GUI Quick tab are to include Airspeed (m/s), Satellite Count, Bat Used (mAh), Altitude (m), Waypoint Number, and Distance Traveled (m).

Figure 40. Screenshot of the telemetry data on Mission Planner's GUI

5.5.4 After Flight

To ensure proper power down first disconnect the Pi, kill the telemetry link through the ground station, and then unplug battery. If a transmitter is used, be sure to switch it off as well. Data and the telemetry recording are automatically saved on the flight controlled SD card and the ground station. If any air traffic management systems are being used, be sure to update mission results.

5.6 Performance Specifications

EcoSoar should take off at a weight of 1.5 kg. The empty weight varies depending on print quality and build details. The payload comes out to be the difference between 1.5 kg and the empty weight. The aircraft can fly at a velocity of 14 m/s for imagery missions or 18 m/s for delivery missions. The range and endurance max out around 25 km and 30 minutes. Performance specifications and flight experiment results for glide tests are shown in Table 8 and 9. The glide ratio comes out to be 4.53, which is expected from homebuilt tailless UAV. (Kraft, 2017)

Table 8. *EcoSoar* aircraft characteristics

EcoSoar Flight Characteristics	
Weight	~1.4 kg
Payload	~0.1 kg
Range	25 km
Endurance	30 mins
Cruise Speed	14 m/s or 18 m/s
Cruise Altitude	60-100 m

Table 9. Data showing unpowered altitude and distance start and end points and respective lift-to-drag ratio

Altitude Δ (m)	Distance Δ (m)	L/D
122	574	4.70
125.6	570.3	4.54
123.5	561.9	4.55
118.1	540	4.57
83.8	357.7	4.27
112.8	557.6	4.94
115.3	475.9	4.13

Chaper 6. Proof of Concept in Malawi Drone Testing Corridor

New technologies spur new solutions to everyday challenges. Drone technology through *EcoSoar* could be used to tackle issues such as remote medicine transport and environmental or infrastructure monitoring in developing nations. Other applications could be thought of after

introducing drone technology to such communities since they know their problems more than anyone does. An opportunity to test the merits of *EcoSoar* for some of these cases came when visiting UNICEF's drone-testing corridor in Kasungu, Malawi. The research airspace was opened to evaluate the potential solutions of UAV technology.

6.1 Test Results

A week trip was made to Malawi, Africa to participate in the UNICEF run drone-testing corridor. The schedule split into two days of workshop and three days of flying. Thirteen locals, both students and entrepreneurs, attended the workshop where a USL team ran through the process of building and operating EcoSoar. There were only two instructors with experience, but the 13 workshop members easily grasped the building techniques. The video series was available for sanity checks but no one felt that watching was necessary. The templates proved to be intuitive when comparing them to pictures of finished wings. No one struggled with alignment of parts or initial part placement. Overall, the building procedures were well adhered to and the resulting airframes were all capable of flight.

Several issues arose during the flight tests that could have been avoided. The aircraft brought from the States, EcoIR, malfunctioned due to a receiver connection coming undone. EcoIR glided down surprisingly smooth after loss of control, proving the stability of the design and resilience of the airframe. It was even put back in the air later that same day. Out of the five locally made aircraft, one crashed due to pilot error on launch and another crashed due to faulty control based on finicky airspeed data. Another aircraft was grounded because of odd behavior by oscillating in flight; inspection afterwards showed that the airspeed wire must have broken on launch. This oscillating behavior has been seen before in prototypes that attempted to fly

autonomously without airspeed. Another aircraft unfortunately never had the turn due to time restrictions and inclement weather.

Figure 41. Photo of Malawi group and all versions of *EcoSoar* made

The big story from the trip comes from the one aircraft that managed to overcome all the others' misfortunes. Built by students from Malawi University of Science and Technology (MUST), the aircraft appropriately nicknamed EcoMUST flew one piloted flight and two completely autonomous flights. One of the autonomous flights was a 19 km beyond line of sight test mission where the aircraft flew a simulated medical delivery from a village clinic back to the research facility base at Kasungu airport. An operator traveled to the clinic, without a pilot, and launched EcoMust into its autonomous mission. The flight mission is shown in Figure (37) and the final flight path is below in Figure (42). The pilot remained on the receiving end, without cellphone or any indication the aircraft was on its way, just in case the landing went wrong. Eventually a low buzz was heard and EcoMUST properly followed its decent path to land fully autonomously.

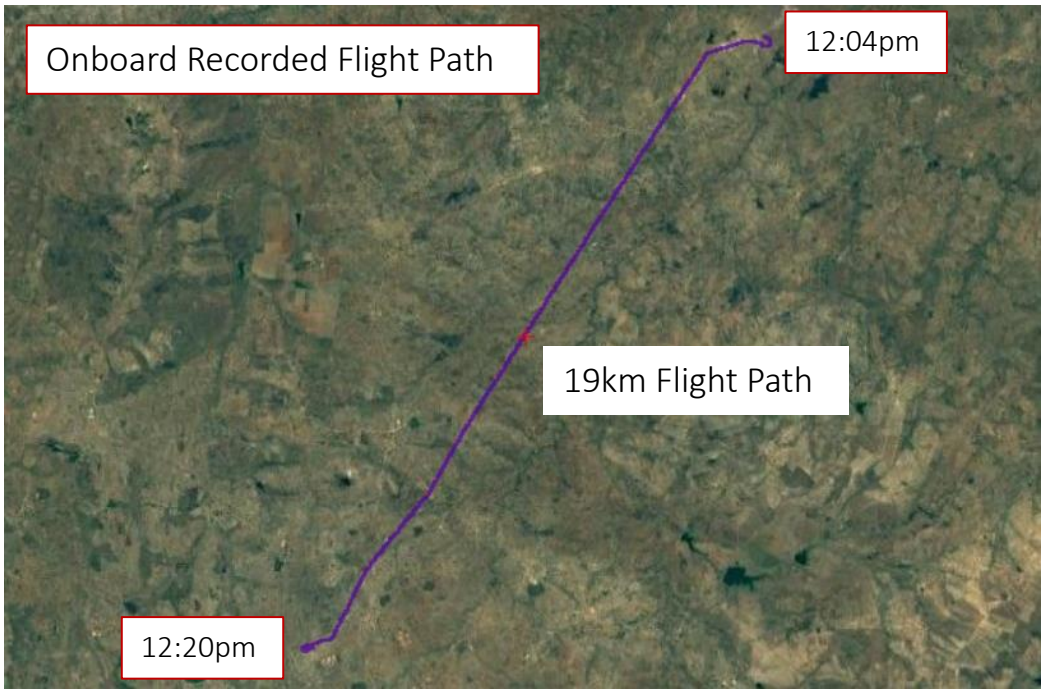

Figure 42. Flight path of EcoMUST's autonomous BLOS medical transport mission

6.2 Lessons Learned

The biggest issues in the production process occurred with glue volume. The instructions did not clearly state glue amounts and some Malawi builds suffered because of this. The biggest issues with flight operations came in the minor details of preparing for mass production. Everything the team had done up to this point all dealt with only one aircraft at a time. Every component brought to Africa was checked for quality control, yet an airspeed wire joint ripped, a temperamental flight controller misread airspeed data, and a loose connection of a receiver came apart during aircraft launch. The instructions now include sections on gluing down wires to prevent unwanted tensions on wires within the wings. The flight controller has many knockoffs on the market, and though reliable in prototyping efforts, the potential for one out of six flight controllers being faulty is tragic. Signs such as climbing airspeed when the aircraft is stationary now serve as warnings for defective flight controllers. Out of flight controllers brought to Africa, the most reliable is the HkPilot32.

Chaper 7. EcoSoar Design Upgrade: Optimization and Flight Validation

The brute force through which EcoSoar was developed left out aspects of design engineering which could result in better flight performance. The wing design priority fell on the feasibility and simplicity of construction, leaving the wing aerodynamic design as a secondary process. With inspiration from the new and extremely efficient Lockheed Martin Blend-Wing Body, shown in Figure (43), an aerodynamic design analysis was desired. After the creation of multiple posterboard builds, the possibilities of the manufacturing techniques revealed themselves. Though wing features such as dihedral and twist remained out of the equation, it was hypothesized that the posterboard wings could be made of two panels each – opposed to the one piece of posterboard per wing used for EcoSoar. This would allow for a larger wingspan and area. In attempt to maximize range and increase payload capacity, a study was performed to optimize the lift-to-drag ratio of realistic geometry for two panel posterboard wings.

Figure 43. Lockheed Martin's hybrid wing body concept (NASA, 2017)

7.1 Optimization Criteria

By freezing the electronics and airframe configuration, the only variable to change is the shape of the wings. Span is limited by constraining the two sections of each wing to their own sheet of 20”x30” posterboard. Other constraints were developed using experience from previous posterboard builds. Some models showed obvious bending stress (creases in the foam after flight) concentrated where the main spar ends due to wing sweep. To prevent unwanted bending, it is desired for the new design to utilize a spar that traverses the entire span. This constrains the geometry in such a way a spar can go from wing tip to wing tip.

7.2 Design Variables

The wing planform geometry will be the only parameters changing throughout the analysis. Chord, span and sweep values will vary while calculating and comparing lift and induced drag. By introducing taper ratios, the amount of chord variables reduces from three to two. Figure (44) shows how design variables are defined.

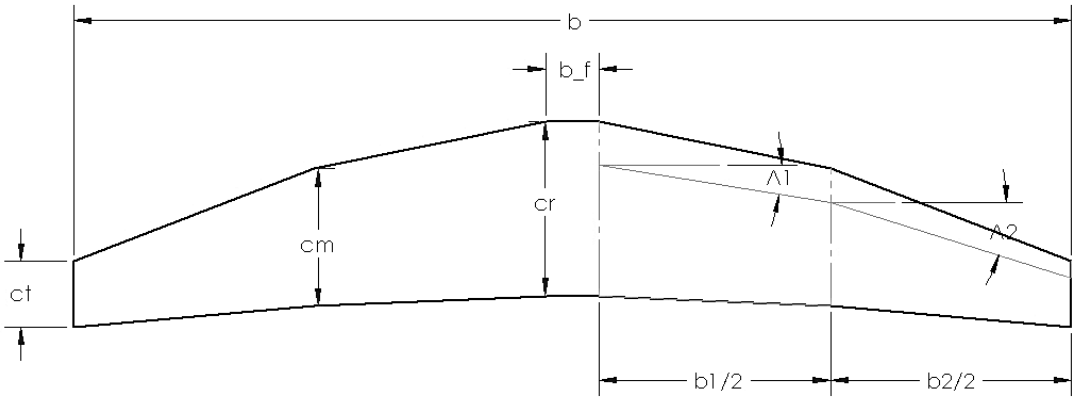

Figure 44. Top-view of upgraded flying wing planform showing design variables

The design variables are:

- Taper ratio ($\lambda_1 = \frac{C_r}{C_m},\ \lambda 2 = \frac{C_m}{C_t}$)
- Where c_r, c_m, and c_t are the root, middle, and tip chord values respectively

- Wing section half spans (b_1, b_2)
- Wing sweep (Λ_1, Λ_2)

In standard notation:

$$x = \begin{bmatrix} x_1 \\ x_2 \\ x_3 \\ x_4 \\ x_5 \\ x_6 \end{bmatrix} = \begin{bmatrix} \lambda_1 \\ \lambda_2 \\ b_1 \\ b_2 \\ \Lambda_1 \\ \Lambda_2 \end{bmatrix}$$

The subscript denotes wing section; inboard is section 1 and outboard is section 2 as depicted by Figure (44).

7.3 Constraints

The main constraining forces of planform geometry come from the building materials and techniques. The posterboard confines the wing shape such that the six-sided 2D panel must fit on a 30”x20” rectangle. Table 10 shows a list of values derived from using posterboard.

Table 10. Constant constraints used in two-panel wing analysis

Variable	Value	Description
c_r	0.2794	meters, chord at the root
b =	0.84	meters, half span
$c_{m,min}$	0.0931333	meters, min mid root chord length
$c_{m,max}$	0.2794	meters, max mid root chord length
$c_{t,max}$	0.508	meters, max tip root chord length
$b_{1,max}$	0.84	meters, max inboard span
$b_{2,max}$	0.84	meters, max outboard span
$\lambda_{1,max}$	1	max inboard taper ratio
$\lambda_{2,max}$	1	max outboard taper ratio
$\Lambda_{1,max}$	π/3	radians, max inboard sweep
$\Lambda_{2,max}$	π/3	radians, max outboard sweep

To constrain the wing geometry such that a spar can transverse from wing tip to wing tip, assuming the spar can still fit in the wing at 75% of the root chord from the nose, the following equation was created:

$$g_1 = x_3 * \tan(x_5) + x_4 * \tan(x_6) - \frac{3}{4}c_r = 0$$

7.4 Approach and Analysis

To compare flying wing geometries, aerodynamic analysis code is paired with MATLAB optimization algorithms. Code, provided by Virginia Tech Professor William Devenport, was modified to model and analyze the two-panel wing geometry. First, wing surfaces are defined and used to create a 3D mesh in "wing.m" (Devenport & Standridge, 2016b). Design variables and number of mesh segments are input into this function, which then outputs the arrays necessary to define the wing. The wing created is nondimensionalized by defining the root chord as one. Results are scalable by defining a new root chord dimension.

Second, wing mesh is input to "DoubletPanel3DWing.m" (Devenport & Standridge, 2016a) for analysis. This function is a 3D ideal flow solver that outputs aerodynamic force coefficients. To optimize the planform geometry for a maximum range, the lift-to-drag ratio is analyzed using MATLAB optimization tools.

7.5 Optimization with MATLAB's "fmincon"

MATLAB's "fmincon" function attempts to minimize an objective function considering the input constraints and initial guesses. Constraints can be either linear in matrix form or nonlinear in function form. Input options allow the user to change algorithms from a list of built in methods. Since maximizing lift-to-drag is the same as minimizing drag-to-lift, a cost function is created with the inverse output of DoubletPanel3dWing.m:

$$C_D/C_L(\lambda_1, \lambda_2, b_1, b_2, \Lambda_1, \Lambda_2)$$

The optimized design variables are called in MATLAB by:

$$x = fmincon(\frac{C_D}{C_L}, x0, A, b, Aeq, beq, lb, ub, nonlcon)$$

Where x0 is the initial guess and the rest hold the constraints mentioned in section 7.3.

7.6 Optimization Results and Discussion

Numerical optimization is performed using Sequential Quadratic Programming (SQP) and Interior Point method. These numerical methods are applied using MATLAB's fmincon function. All results shown are dimensionalized from code output by multiplying by EcoSoar's root chord of 11 in (0.28 m). The results from MATLAB's fmincon function with SQP algorithm:

$$f(x) = \frac{L}{D} = 118.9; \quad \begin{bmatrix} x_1 \\ x_2 \\ x_3 \\ x_4 \\ x_5 \\ x_6 \end{bmatrix} = \begin{bmatrix} \lambda_1 \\ \lambda_2 \\ b_1 \\ b_2 \\ \Lambda_1 \\ \Lambda_2 \end{bmatrix} = \begin{bmatrix} 0.6795 \\ 0.3393 \\ 0.9220m \\ 0.7560m \\ 0.0000° \\ 15.47° \end{bmatrix}$$

This run ended in 25 iterations and gave the message "Local minimum possible. Constraints satisfied."

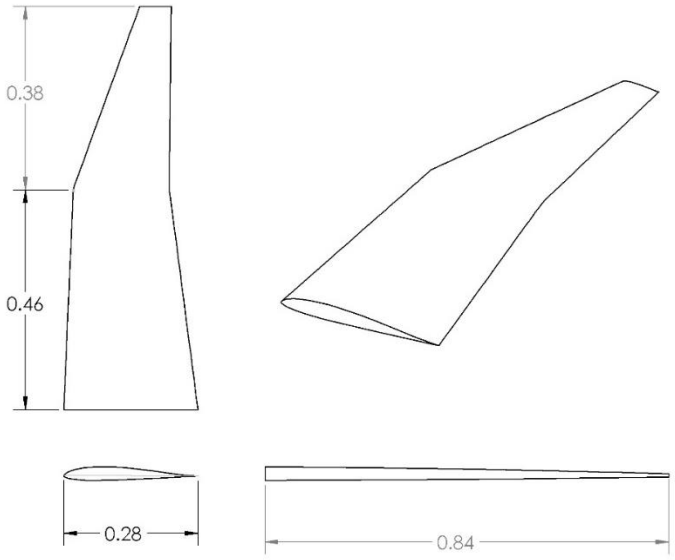

Figure 45. SQP result geometry, showing dimensions in meters

The results from MATLAB's fmincon function with Interior-Point algorithm:

$$f(x) = \frac{L}{D} = 116.6; \quad \begin{bmatrix} x_1 \\ x_2 \\ x_3 \\ x_4 \\ x_5 \\ x_6 \end{bmatrix} = \begin{bmatrix} \lambda_1 \\ \lambda_2 \\ b_1 \\ b_2 \\ \Lambda_1 \\ \Lambda_2 \end{bmatrix} = \begin{bmatrix} 0.7238 \\ 0.3082 \\ 0.8541m \\ 0.7990m \\ 2.750° \\ 10.77° \end{bmatrix}$$

This run ended in 37 iterations and gave the message "Local minimum possible. Constraints satisfied."

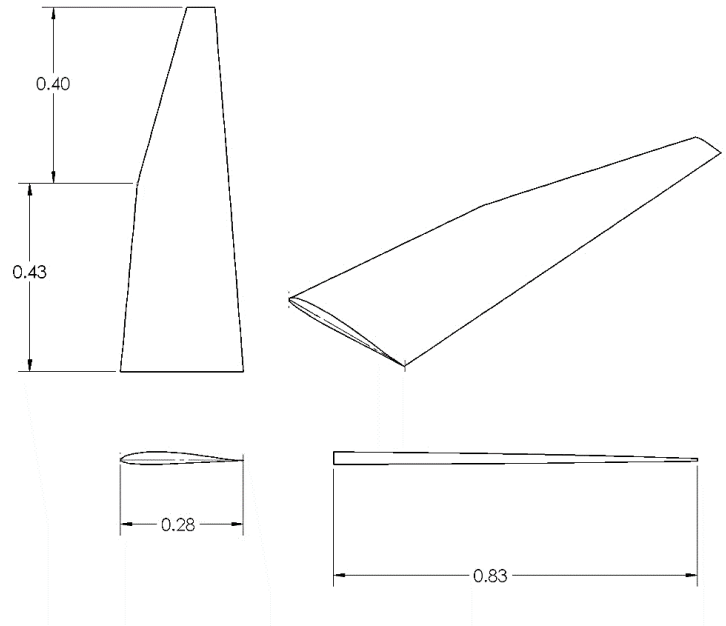

Figure 46. Interior-point result geometry, showing dimensions in meters

There is an obvious difference in the two results. SQP found a slightly better solution in fewer iterations. The difference in results could be due to a low mesh count. For each run, the amount of spanwise panels was set to 50. For example, when the panel count is increased to 200, the L/D values (though within 1%) change. The iteration output of each method is low meaning the major time consumer is the aerodynamic analysis. Each optimization run took roughly 6 hours, by increasing the mesh count this time would grow absurdly. Another point to make is that the L/D values obtained are unrealistic. The doublet panel method does not take into account parasitic drag. Meaning the ratios are only valuable when compared to each other.

Another difference in the method solutions is due to the inherit characteristics of the algorithms. Interior-point is a linear approximation solver, looking for point inside the feasible domain. Where SQP is a quadratic solver that searches along the constraint surfaces. These solutions could very well be on track to the same critical point, though the interior-point method will always fall short. For this reason, further optimization results are done with only SQP.

Upon further consideration, it would be feasible to create a wing with an outboard panel consisting of some spar and the rest posterboard beams. Meaning the spar would end somewhere within the outboard panels as opposed to the wingtips. The results from MATLAB's fmincon function with SQP algorithm without the spar constraint g_1:

$$f(x) = \frac{L}{D} = 244.7; \qquad x = \begin{bmatrix} \lambda_1 \\ \lambda_2 \\ b_1 \\ b_2 \\ \Lambda_1 \\ \Lambda_2 \end{bmatrix} = \begin{bmatrix} 0.7236 \\ 0.4488 \\ 0.8400m \\ 0.8400m \\ 10.20° \\ 36.04° \end{bmatrix}$$

This run ended in 23 iterations and gave the message "Local minimum possible. Constraints satisfied."

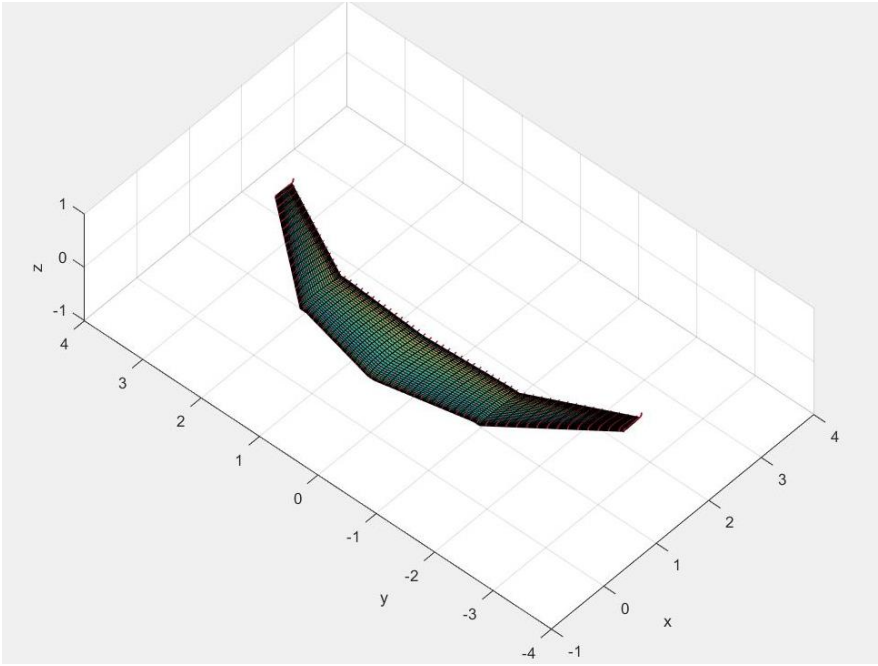

Figure 47. Nondimensional SQP results without spar constraint

This last case yields a significantly higher L/D ratio than other results. The idea to have a full span spar is ideal to keep the construction process simple. However, the point of this study is

to improve the aerodynamic characteristics of EcoSoar. The design variables from this last case are used to build a prototype to compare with EcoSoar using flight experiments.

7.7 "EcoZ" Prototyping and Flight Validation

To rapidly prototype a new wing geometry, it was decided to use the same fuselage and wing root parts from EcoSoar. This root chord of 0.28 m results in the dimensions shown in Figure (48).

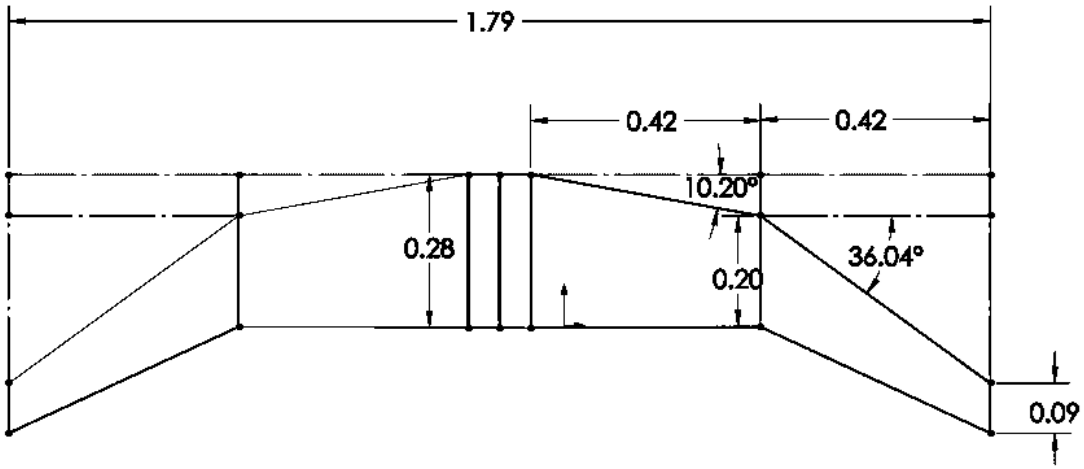

Figure 48. Drawing of EcoZ planform, dimensions in meters

These dimensions were used to create an AVL model to determine total weight and cruise speed. The posterboard wing will have different characteristics but the AVL results allow for a rough flight envelope. Desired cruise speed is 14 m/s to allow camera system adequate image overlap for image stitching. However, faster speeds could result in larger payloads. Both cases are considered since EcoSoar is a multifunction platform. A maximum mass of 2.5 kg is used due to launch dynamics and the bungee used. All cruise angles of attack fall under the MH60 stall of 12° and the typical EcoSoar stall angle of 10°. This does not validate EcoZ's flight capabilities but acts as a sanity check of where the total weight of the aircraft should be. Also

important to note, EcoZ has a 37% increase in lift-to-drag ratio when compared to EcoSoar. The AVL data can be seen in Figures (49-50).

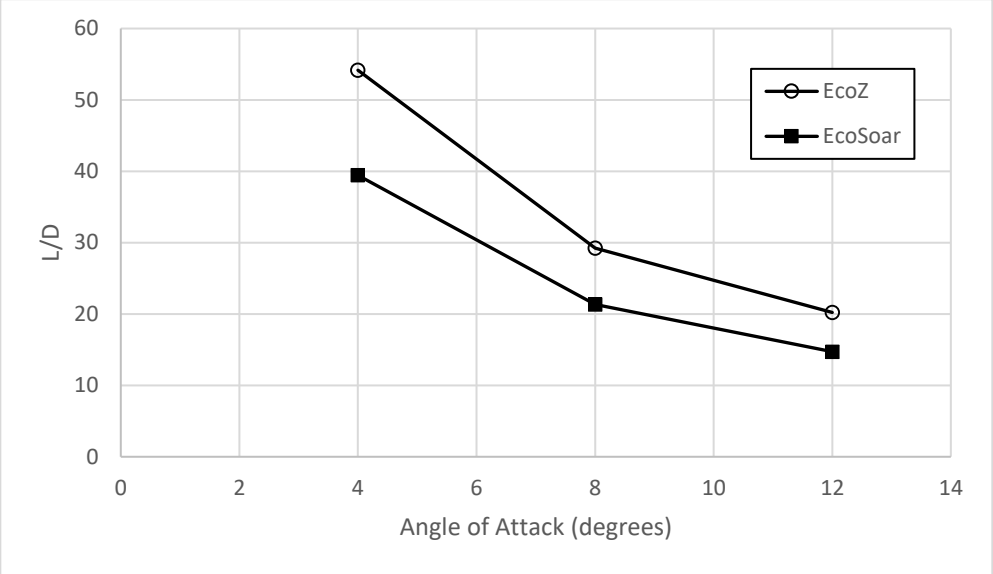

Figure 49. AVL results comparing L/D of EcoSoar and EcoZ at different angles of attack

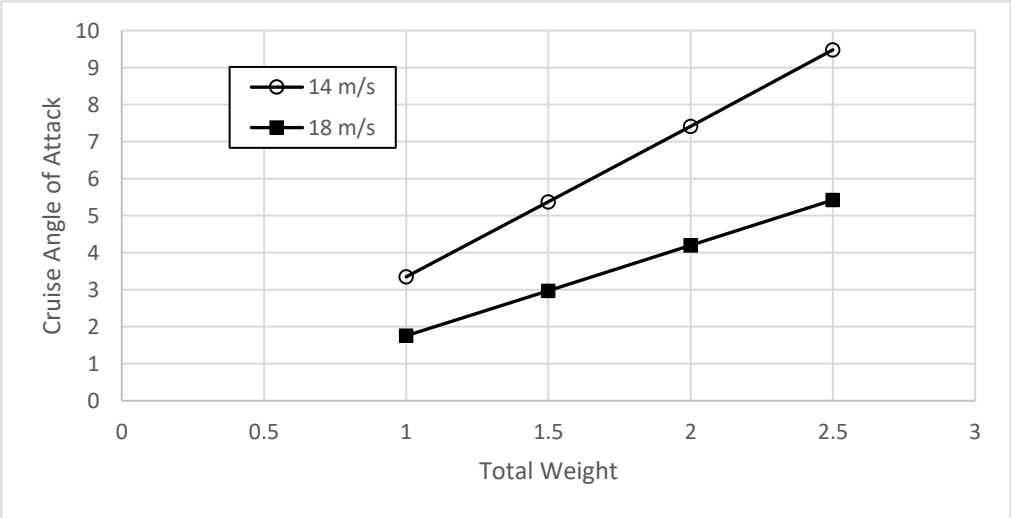

Figure 50. AVL results showing EcoZ's cruise angle of attack at different total weights

Templates were generated using the CAD sketches shown in Figures (51-52). The control surfaces were not included in templates to allow for user freedom when sizing control surface.

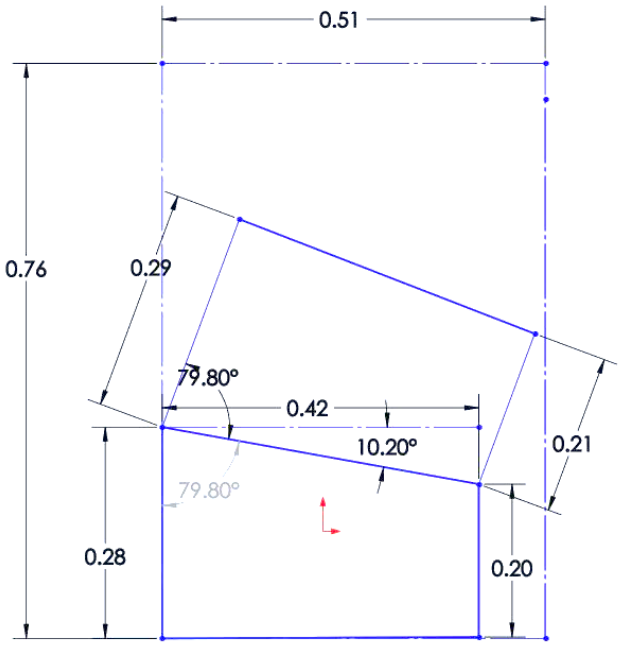

Figure 51. CAD sketch of inboard panel template, dimensions in meters

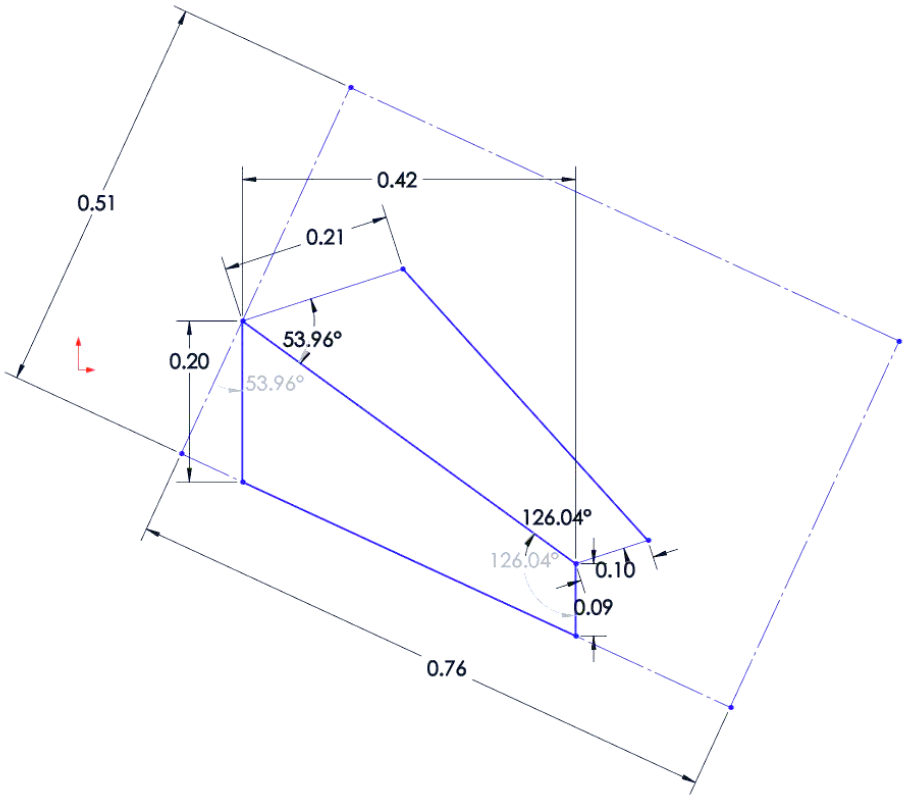

Figure 52. CAD sketch of outboard panel template, dimensions in meters

The EcoZ construction process mimicked a lot from EcoSoar, though replaces leading edge supports and servoribs with foam counterparts. Special attention was given to region where panels meet in order to ensure loads from outboard panel are transferred to spar. Control surfaces are sized to be the same as the width of tape used, which comes out to be 4.8 cm (1.9 in) and right in the historically approved control surface area of 11.7% the wing area. This made for convenient marking of control surface hinge and thus easy control horn installation. They are constrained to the outboard panel in attempt to reduce drag on inboard panel. The trailing edge of the inboard panel now comes to a point.

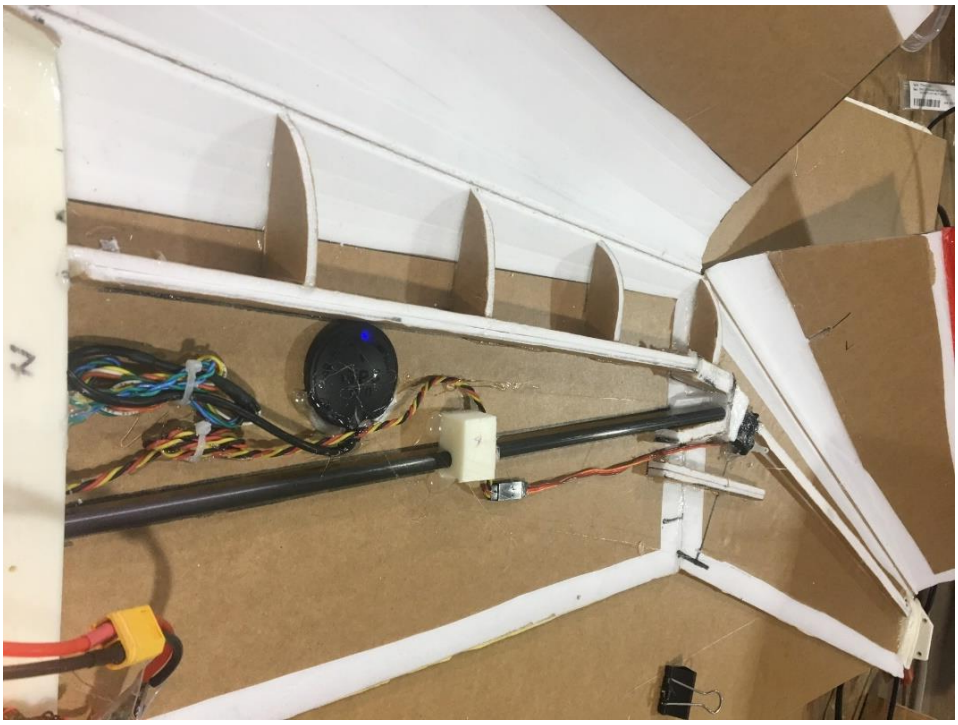

Figure 53. Inside of right wing

The EcoZ build ended up weighing 1.43 kg, using scaling factors from EcoSoar (AVL to actual flight performance) EcoZ can potentially carry 2.25 kg at 16 m/s. This, plus the AVL produced efficiency increase of 37% puts the potential range at 34 km. All while only costing two extra pieces of posterboard or exactly $4 more than EcoSoar.

Table 11. EcoZ Flight Characteristics from construction and AVL

EcoZ Flight Characteristics	
Mass (empty)	1.43kg
Payload	0.72kg
Cruise Velocity	16m/s
Range	33 km (66 km with 2nd 0.35kg battery)
Cost	~$352

Figure 54. EcoZ on the day of its maiden flight

Though the electronics are the same as EcoSoar, the control mechanisms are much too different to carry flight controller gains over across builds. However, it was decided that EcoSoar control gains could act as a starting point for EcoZ. The first test flight was conducted in assisted flight mode FBWA using EcoSoar control gains to validate flight capabilities. The aircraft's CG moved forward closer to the bungee anchor point. Meaning the aircraft is much more sensitive in pitch when pulled from below. This was taken into consideration before launch and the launch rung used was #1, the one closest to the fuselage. Still, the first launch attempt was a failure, fortunately with minimal damage, due to stall while still on the bungee line.

The next launch attempt was done with full elevator down to keep the aircraft level. This launch was a success. The pilot quickly noticed gains were causing the aircraft to overcorrect so the flight mode was switched to AUTOTUNE. Once comfortable, glide slope tests were performed. This is where the pilot climbs, kills the motor, and glides down as far as possible. Stored flight data is later accessed to find altitude and distance when motor is off. The results are shown below in Table 12.

Table 12. Data showing unpowered altitude and distance start and end points

Altitude Δ (m)	Distance Δ (m)	L/D
109	692.5	6.35
102	653	6.40
123	829	6.74
63.5	464	7.31

These glide slopes average out to be 6.7, which is 37% more efficient than results from EcoSoar glide slope tests resulting in a ratio of 4.9. These experiments seem to validate the AVL lift-to-drag ratio comparison shown in Figure (49).

EcoZ's second flight was a maximum range mission. The goal was to run the aircraft as long as safely possible in order to validate the range increase. An autonomous mission was desired, however, the aircraft oscillations were too frequent for the AUTOTUNE process to develop reliable gains. The pilot instead flew in FBWA for over 30 minutes while a ground station operator monitored airspeed, current, and voltage. The mission resulted in a final range of 32.98 km and an endurance of 1964 s (32.7 min) with a 9.91V battery as shown by the telemetry screenshot in Figure (55).

Figure 55. Screenshot of the final telemetry data from EcoZ's second mission

The airframe was determined to be more aerodynamically efficient than EcoSoar even though the range mission was remotely piloted due to odd flight behavior. These oscillations experienced in flight are thought to be structure induced. The bending due to inadequate load transferring during control surface deflections could result in the observed behavior. Stiffer aircraft wings could lead to reliable control gains and therefore autonomy. Flight testing experience shows that autonomous missions draw far less current than piloted ones. Therefore, it is predicted a better wing structure could lead to an autonomous EcoZ and can travel even further than 33 km.

Chaper 8. Conclusions and Future Work

A prototype UAV has been refined through construction techniques and flight experiments. The fully autonomous unmanned aerial vehicle (UAV), named EcoSoar, is a viable business option for local entrepreneurs in low-resource communities. 3D printed parts have been

integrated to the design to aid in airfoil conformity, manufacturing simplicity, and structural support. The system was tested in Malawi, Africa and proved that local fabrication, operation, and maintenance of the aircraft are all possible. EcoSoar is made with reliable low-cost materials and electronics costing no more than $350. An upgraded wing geometry planform was computed and built in order to optimize vehicle range. Aerodynamic software AVL calculations and flight experiment data agree that the new wings increase the aircraft efficiency around 37%.

Future work could include strengthening control surfaces such that they could come to a point; it is believed this would improve drag results. Another system improvement could be the creation of a more reliable launcher. There will be an on-going effort to gather all production and operation needs into a master folder, which can be found here. It is the team's desire to make *EcoSoar* an open source DIY drone kit.

References

Amukele, T., Ness, P. M., Tobian, A. A. R., Boyd, J., & Street, J. (2017). Drone Amukele, T., Ness, P. M., Tobian, A. A. R., Boyd, J., & Street, J. (2017). Drone transportation of blood products. *Transfusion, 57*(3), 582-588. doi:10.1111/trf.13900

Amukele, T. K., Sokoll, L. J., Pepper, D., Howard, D. P., & Street, J. (2015). Can Unmanned Aerial Systems (Drones) Be Used for the Routine Transport of Chemistry, Hematology, and Coagulation Laboratory Specimens? *PLOS ONE, 10*(7), e0134020. doi:10.1371/journal.pone.0134020

Devenport, W., & Standridge, Z. (2016a). DoubletPanel3dWing.m MATLAB: Virginia (1.) Tech.

Devenport, W., & Standridge, Z. (2016b). Wing.m MATLAB: Virginia Tech.

Drela, M., & Youngren, H. (2004). Athena Vortex Lattice: MIT. Retrieved from web.mit.edu/drela/Public/web/avl/

Haidari, L. A., Brown, S. T., Ferguson, M., Bancroft, E., Spiker, M., Wilcox, A., . . . Lee, B. Y. (2016). The economic and operational value of using drones to transport vaccines. *Vaccine, 34*(34), 4062-4067. doi:10.1016/j.vaccine.2016.06.022

Hall, N. (Producer). (2015). Force Balance. Retrieved from https://www.grc.nasa.gov/www/k-12/airplane/tunbal.html

Hepperle, M. (2004). MH 60 https://www.mh-aerotools.de/airfoils/mh60koo.htm

2Kamk (3.) wamba, W., & Mealer, B. (2009). Planting Trees and Moving Windmills in Malawi. Retrieved from https://www.huffingtonpost.com/william-kamkwamba/planting-trees-and-moving_b_302647.html

Kolodny, L. (2016a). A test flight with Zipline, makers of humanitarian delivery drones. In. New York: AOL Inc.

Kolodny, L. (2016b). Zipline drones airdrop medical supplies to African villages. In. New York: AOL Inc.

Kraft, T. E. (2017). *Extended Range Aerial Delivery Using an Unpowered Autonomous Tailless UAV*. (Dissertation/Thesis), ProQuest Dissertations Publishing

Mader, C., & Martins, J. (2012). *Optimal Flying Wings: A Numerical Optimization Study*, Reston.

MH 60 10.08% (mh60-il) Polars. (2018). Available from Xfoil http://airfoiltools.com/airfoil/details?airfoil=mh60-il#polars

Mitchell, C. (2017, 2017 August-September). Malawi's drone corridor challenges skepticism towards UAVs: stringent regulations restrict the use of drones in many parts of Africa, but a new scheme demonstrates their potential for humanitarian work. *African Business*, 86+.

NASA, L. M. A. C. (Producer). (2017). NASA Takes Next Step in Green Aviation X-planes Plans. Retrieved from https://www.nasa.gov/aero/nasa-green-aviation-x-planes

Nelsen, E., & Stowe, M. (2016). Project Wing partners with Virginia Tech to test delivery by unmanned aircraft [Press release]. Retrieved from https://vtnews.vt.edu/articles/2016/09/ictas-maapprojectwing.html

Oborne, M. (2016). Mission Planner (Version 1.3.48). ArduPilot.org. Retrieved from http://ardupilot.org/planner/docs/mission-planner-overview.html

Rinaudo, K. (2018). How Zipline Works. Retrieved from http://www.flyzipline.com/service/

Scott, J. E., & Scott, C. H. (2017). *Drone Delivery Models for Healthcare.* Paper presented at the 50th Hawaii International Conference on System Sciences.

Templeton, D., & David, T. DRONE DELIVERY OF VACCINES WOULD BE COST-EFFECTIVE. *Pittsburgh post-gazette (Pittsburgh, Pa. 1978).*

Vandevelde, C., Wyffels, F., Ciocci, M.-C., Vanderborght, B., & Saldien, J. (2016). Design and evaluation of a DIY construction system for educational robot kits. *International Journal of Technology and Design Education, 26*(4), 521-540. doi:10.1007/s10798-015-9324-1

Weerdt, R. V. d. (2016). Contraceptive delivery by drone to African women. *Appropriate Technology, 43*(2), 10.